Accepted Manuscript

Instabilities in the axisymmetric magnetoelastic deformation of a cylindrical membrane

Narravula Harshavardhan Reddy, Prashant Saxena

Please cite this article as: Narravula Harshavardhan Reddy, Prashant Saxena, Instabilities in the axisymmetric magnetoelastic deformation of a cylindrical membrane, *International Journal of Solids and Structures* (2017), doi: 10.1016/j.ijsolstr.2017.12.015

Instabilities in the axisymmetric magnetoelastic deformation of a cylindrical membrane

Narravula Harshavardhan Reddy, Prashant Saxena[*]

Department of Mechanical & Aerospace Engineering,

Indian Institute of Technology Hyderabad

Kandi, Sangareddy 502285, Telangana, India

Abstract

We study the inflation of a weakly magnetizable isotropic incompressible cylindrical membrane and the effects of an external magnetic field generated by a current carrying wire placed along the axis of cylinder. A variational formulation based on magnetization is used and the computational results obtained by using four elastic constitutive models (neo-Hookean, Mooney–Rivlin, Ogden, and Arruda–Boyce) are studied and compared. Cylinders of various aspect ratios are studied in each case. Our study shows that the external magnetic field alters the elastic limit point, does not lead to equilibrium solutions below certain value of internal pressure, and can give rise to multiple equilibrium states for a given value of pressure. Presence of magnetic limit point, a phenomenon recently reported in the literature is reconfirmed. Magnetic limit point is a state where a further strengthening of the applied magnetic field at a given pressure does not yield any static equilibrium state. In this case it is detected when the cylindrical membrane deflates into the volume enclosed by itself. We also observe a quadratic relation between the defined magnetic energy parameter and the internal pressure at the magnetic limit point. Relaxed form of the strain energy density is used to account for wrinkling in this case of inward inflation. A finite difference method coupled with an arc-length technique is used for the computations and the stability of the solution is determined from the second variation.

Keywords: magnetoelasticity; finite deformation; membrane; limit point; wrinkling

Mathematics Subject Classification: 74B20, 74F15, 74G60, 74K15

[*]Corresponding author. Email: prashant_saxena@iith.ac.in, Phone: +91 40 2301 6151

1 Introduction

Studying the behaviour of nonlinear elastic membranes is of paramount importance given their key role in safety, structural and aerospace applications. Several biological materials like tissues, cell walls and skin also fall under this material category. Presence of material and geometric nonlinearity in the study of such problems make them both interesting and complex. While simply connected and axisymmetric geometries can be studied analytically, computational techniques are required to study most other problems. For example, see (Yang and Feng, 1970) where a direct integration method is used to obtain the governing equations for axi-symmetric deformations, (Grossman, 1991a,b, 1994) for non-axisymmetric deformations of inflatable reflectors for space applications, and (Khayat and Derdouri, 1994a,b) for both axisymmetric and non-axisymmetric deformations of cylindrical membranes.

Study of nonlinear elastic cylindrical membranes find applications in areas such as biomedical equipments (Leone, 1994), in thermoforming, balloons and parachutes, blow moulding (Khayat and Derdouri, 1994a,b). To quote a few examples of free and confined inflation of cylindrical membranes: Kydoniefs and Spencer (1969) studied axisymmetric deformations using Mooney-Rivlin material model; Skala (1970) studied propagation of bulging with neo-Hookean and Mooney-Rivlin models; Haughton and Ogden (1979) studied bifurcation in pre-stretched thin tubes using Ogden's model; Wriggers and Taylor (1990) developed a finite element model coupled with arc-length and Newton's methods for axisymmetric deformations; Kyriakides and Yu-Chung (1991) studied, experimentally and analytically, bulging and bifurcation using Ogden's constitutive model; Khayat et al. (1993) worked on both free and confined inflation of cylindrical membranes of various length to radius ratios using neo-Hookean and Mooney-Rivlin models; Pamplona et al. (2001) studied analytically, and verified with experiments, fluid-filled, pre-stretched cylindrical membranes using neo-Hookean model; Pamplona et al. (2006) worked on neo-Hookean and Mooney-Rivlin material membranes pressured with a gas using a commercial finite element software and experiments; Patil et al. (2014) studied free and adhesive contact constrained inflation using Mooney-Rivlin hyperelastic material model; Patil et al. (2015b) studied wrinkling in cylindrical membranes with non-uniform thickness using Mooney-Rivlin constitutive model; Patil et al. (2015a) studied fluid-loaded, pre-stretched membranes using neo-Hookean material model. However, none of these researchers studied inward inflation of a cylindrical membrane caused by higher pressure outside the cylinder. In the current study, we will try to fill this gap.

Study of inward inflation requires one to consider the possibility of wrinkling. Wrinkling is a form of buckling commonly observed in thin shells or membranes undergoing compressive stresses. In plane loading can lead to out of plane deformations when the structure experiences a critical state of compressive stresses. Various approaches have been taken to study wrinkling in structures, notable among them being the tension field theory. Tension field theory assumes that one of the principal stresses goes to zero in the event of wrinkling and the crests and troughs of the wrinkles align with the direction of the positive principal stress. In other words, the infinitesimally small wrinkles are perpendicular to the 'tension lines' (Pipkin, 1986). Note that since membranes are assumed to have zero stiffness, this theory is unable to predict a physical dimension like amplitude or wavelength of wrinkles. Various authors have extended this theory to simulate wrinkles analytically, for example, by introducing variable poisson's ratio (Stein and Hedgepeth, 1961); by treating the wrinkles as material anisotropy (Mansfield, 1981). Wu (1974) assumed that the membrane is absolutely a no-compression structure with zero bending stiffness and that the infinitesimal wrinkles are uniformly distributed over a so-called 'pseudosurface'. It is worth recalling that it is the bending stiffness of the membrane that decides the amplitude and wavelength of wrinkles. Any absence of it should give only infinitesimally small wrinkles.

Only kinematic analyses had been conducted until Pipkin (1986) proposed that the geometric nonlinearity be interpreted as a nonlinearity in the constitutive relations. He introduced a 'relaxed energy density' that automatically considers wrinkling and gives an average solution over the wrinkled domain or in other words, over Wu (1974)'s pseudo-surface. However, this method was limited to linear elastic thin sheets until Steigmann (1990) extended it to nonlinear isotropic elastic membranes. Haughton and McKay (1995) present some examples to further illustrate Pipkin and Steigmann's tension field theory. Epstein (1999) later showed that anisotropic membranes can also have unique relaxed energy densities. A few analytical studies on wrinkling of nonlinear elastic membranes using the concept of relaxed free energy density have been undertaken by Steigmann and Pipkin (1989); Li and Steigmann (1995a,b), and Patil et al. (2015b). We use the same concept here in our study of a cylindrical membrane.

An important phenomenon to consider during the inflation of membranes is the elastic limit point (or the snap-through) instability. Internal pressure required to stretch the membrane increases until this point and drops afterwards. A rise in the pressure may be seen again in

the case of strain-hardening. A priori knowledge of this critical point is crucial to maintain the deformation of membrane within the acceptable limits. Almost every study on membranes talks about the elastic limit point. For example, see the works by Benedict et al. (1979) on limit point pressures in nonlinear elastic tubes, by Khayat et al. (1992) on cylindrical membranes with a focus on bulging after the limit point, by Alexander (1971) on such a behaviour of spherical rubber balloons under inflation, and more recently by Rudykh et al. (2012) on the snap-through actuation in the case of an electro-active spherical membrane.

Khayat et al. (1992) discuss some difficulties with various numerical techniques while solving nonlinear differential equations governing the deformation of cylindrical membranes. According to them the shooting method becomes unstable due to the nonlinearity and that a finite difference discretization followed by Newton-Raphson method is a good choice for studying deformations of cylindrical membrane. Recently, Patil et al. (2014, 2015a,b) also followed a finite difference scheme. In addition, a cubic extrapolation arc-length technique is utilized to evaluate initial guesses for further iterations using the solutions from previous iterations. We also note an instance of studying fluid-filled membranes using shooting method by Pamplona et al. (2001). In this study, we follow similar numerical approach as in (Patil et al., 2015a,b).

Magnetoelastic polymers are smart materials that can deform under the influence of an external magnetic field and perturb the surrounding magnetic field when deformed mechanically. They are usually comprised of micron-sized ferromagnetic particles like iron suspended in a polymer matrix. See, for example, the works by Jolly et al. (1996); Farshad and Benine (2004); Gong et al. (2005), and Krautz et al. (2017) for their fabrication and experimental characterization. The individual magnetization vectors due to the ferromagnetic particles tend to align with the external applied magnetic field resulting in a change in macroscopic properties like stiffness and dimensions (Ginder et al., 2002; Böse and Röder, 2009). This phenomenon is exploited in several practical applications such as sensors, actuators, vibration control, dynamic stiffness control, waveguides; see, for example, the papers by Ginder et al. (2001); Böse et al. (2012); Keh et al. (2013); Mayer et al. (2013), and Saxena (2017).

Various theoretical studies on magnetoactive materials have been available in the literature for over five decades. Among the earliest are the works by Truesdell and Toupin (1960); Tiersten (1964); Maugin and Eringen (1972); Pao and Yeh (1973) and Pao (1978) based on the conservation laws for continua (sometimes referred to as the direct approach) and the varia-

tional formulations by Tiersten (1965) and Brown (1966) (sometimes referred to as the indirect approach). Nevertheless, these two approaches give similar governing equations as shown by Kankanala and Triantafyllidis (2004).

These classical theories were later adopted by the likes of Brigadnov and Dorfmann (2003); Dorfmann and Ogden (2003, 2005) and Steigmann (2004) to study large nonlinear deformations of magnetoelastic polymers. The total free energy density in these studies is expressed as a function of deformation gradient and one variable among magnetic flux density, field intensity, magnetostatic scalar and vector potentials, and magnetization per unit mass or volume. Magnetization vector is claimed by Kankanala and Triantafyllidis (2004) to be a more natural choice for an independent magnetic variable since it vanishes outside the material. We use the same choice in the current study. In addition to simple models that treat the magnetoelastic material as an isotropic conservative continuous solid, several advanced models have been proposed to account for additional features. For example, Castañeda and Galipeau (2011); Galipeau and Castañeda (2013) and Chatzigeorgiou et al. (2014) formulated coupled field equations using micromechanics and homogenization; Saxena et al. (2013); Ethiraj and Miehe (2016) and Haldar et al. (2016) modelled energy dissipation due to viscoelasticity; Bustamante (2010); Danas et al. (2012) and Saxena et al. (2014) modelled the anisotropic structure of these polymers. These models have been very useful in various theoretical and computational analysis of instabilities in magnetoelastic bulk media, see for example, the works of Otténio et al. (2008); Kankanala and Triantafyllidis (2008); Rudykh and Bertoldi (2013); Danas and Triantafyllidis (2014); Saxena (2017), and Goshkoderia and Rudykh (2017) to name a few. We, however, restrict ourselves to isotropic and conservative magnetoelastic systems in the current study. Readers may refer to the books by Ogden and Steigmann (2011), and Dorfmann and Ogden (2014) for more elaborate literature survey on magneto- and electro-mechanics.

Very few experimental studies on magnetoelastic membranes can be found in the literature. Raikher et al. (2008) performed experiments on the deformation of a circular magnetoelastic membrane under a uniform magnetic field. In the parallel field of electroelasticity, Fox and Goulbourne (2008) studied the displacement of a circular membrane and its dependence on applied potential difference across the membrane and its frequency; Fox and Goulbourne (2009) and Tews et al. (2003) presented pressure vs chamber volume characteristics; Keplinger et al. (2012) and Li et al. (2013) studied the snap-through instability in the inflation process; Bense et al. (2017) reported buckling of circular dielectric elastomer plates using weakly non-linear

plate equations; Wang et al. (2017) observed bulging in inflating circular dielectric elastomer membranes due to the potential difference applied across the thickness.

The theoretical framework for bulk materials was extended to magnetoelastic membranes by Steigmann (2004) using a formulation based on magnetic field intensity. Barham et al. (2007) later simplified the formulation based on magnetization for weakly magnetized materials i.e., when the magnetic field generated by the material due to its mechanical deformation can be neglected in comparison to the applied magnetic field. The expression for total free energy is split into two terms, one solely depending on the elastic deformation–strain energy density and the other containing both elastic and magnetic terms. Besides simplifying the numerical computation, this eliminates the necessity to work with tediously long expressions for total free energy proposed based on experiments by, for example, Bustamante (2010) and Danas et al. (2012) while allowing us to study the fundamental behaviour of the membranes. Barham et al. (2008) first reported the occurrence of magnetic limit point where the stable and unstable states merge in their study of parametric deformation of a weakly magnetized circular membrane in the presence of a stationary magnetic dipole. We (Reddy and Saxena, 2017) also demonstrated a similar phenomenon in the inflation of a magnetoelastic toroidal membrane with magnetic field generated by a current carrying loop inside. We showed that, for a given magnetic energy parameter, inflation does not start until a certain gas pressure is reached and that for a given internal pressure, no static equilibrium solutions are possible beyond a certain value of the magnetic energy parameter. We now aim to observe a similar behaviour in the inflation of a cylindrical membrane in our current study.

It is important to choose a proper hyperelastic constitutive model since not all models can predict all kinds of behaviours (Khayat et al., 1992; Kanner and Horgan, 2007). For example, neo-Hookean model can not predict strain hardening; most Mooney–Rivlin models can not predict bulging in long cylindrical membranes while neo-Hookean model does (Skala, 1970). Kyriakides and Yu-Chung (1991) showed that Ogden model can predict bulging as well. Even in the case of bulk elasticity, it has been shown that no single model is sufficient to predict the material's behaviour over all ranges of strains. For example, see the attempts at modelling the celebrated data of Treloar (1944) by Boyce and Arruda (2000); Seibert and Schoche (2000); Marckmann and Verron (2006), and Steinmann et al. (2012), among others. A large number of studies on static inflation of membranes used neo-Hookean, Mooney-Rivlin or Ogden constitutive models while those using other phenomenological models or chain network-based models

6

are very few. For instance, Rachik et al. (2001) employed and compared with experiments neo-Hookean, Mooney-Rivlin, Ogden, Van der Waals, Arruda-Boyce and Yeoh models in case of a circular membrane; Verron and Marckmann (2003) used chain network-based models including Arruda-Boyce model to study inflation of spherical and circular membranes; Kanner and Horgan (2007) used limiting chain inextensibility models (Gent and power law) for circular and cylindrical membranes; Gent (1999, 2005) used his model to study inflation of thin and thick walled spherical and cylindrical membranes. We also note that Arruda-Boyce model is widely used for modelling biological polymer materials (Bischoff et al., 2000) and we also test its applicability in predicting various membrane instabilities in the present study.

In this paper, we study the magnetoelastic deformations of a weakly magnetizable cylindrical membrane with fixed ends and the associated instabilities. We recall that weak magnetization refers to the case when the magnetization of the magnetoelastic material does not cause changes in the underlying magnetic field. A stationary current carrying wire is placed along the axis of symmetry to generate a magnetic field in the surrounding space. Four constitutive models of elasticity are used to estimate strain energy density and their behaviours are compared. Relaxed energy density is used to model the material in the case of wrinkling. A finite difference approach is taken for obtaining numerical solutions of the resulting system of ODEs. In addition to the usual bulge and wrinkling instabilities associated with elastic membranes, we also show the occurrence of a magnetic limit point instability as has been predicted in our previous work (Reddy and Saxena, 2017). We also show that multiple stable equilibrium solutions are possible in this coupled magneto-mechanical deformation. In the remainder of this article, Section 2 presents the kinematics of deformation, Section 3 presents the derivation of governing equations, various constitutive models and second variation, Section 4 discusses the relaxed free energy density, Section 5 explains the numerical procedure used, Section 6 discusses the numerical results, and Section 7 concludes the study.

2   Kinematics of deformation

2.1   Problem description

Figure 1 shows the incompressible isotropic nonlinear magnetoelastic cylindrical membrane with initial circular cross-section in its undeformed and deformed configurations. The two ends of the cylinder are covered with rigid discs and no initial stretch is given to the cylinder. We
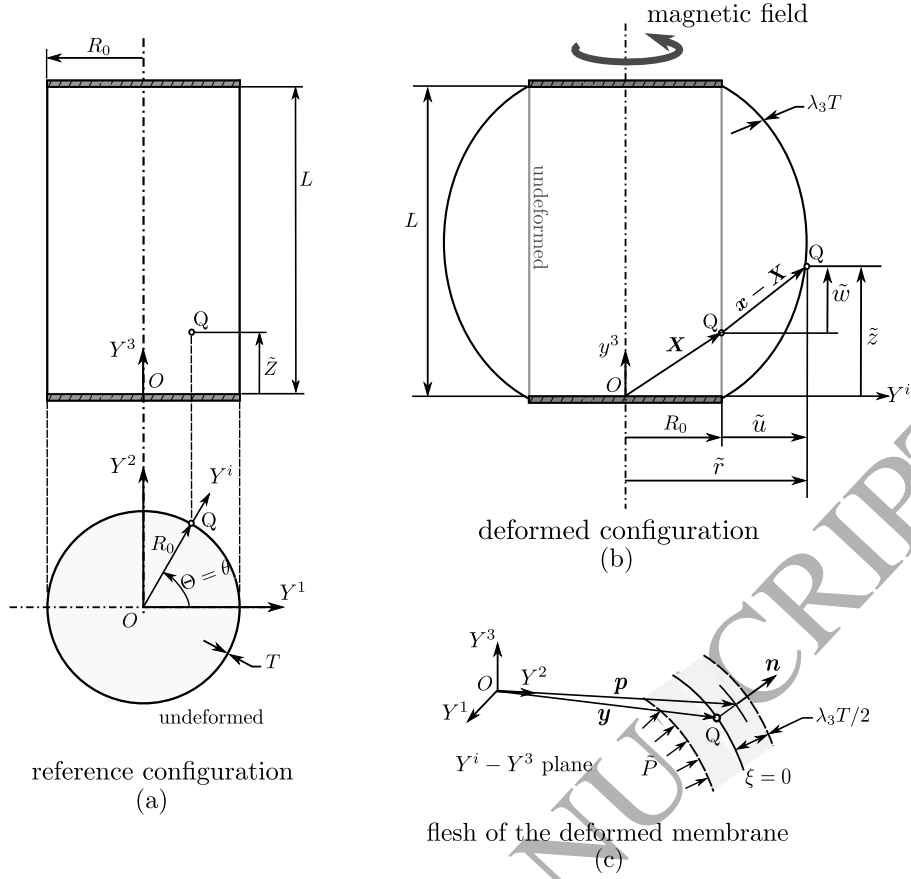
Figure 1: Cylindrical membrane (a) before and (b) after deformation. An azimuthal magnetic field is generated by a current carrying wire along the axis of cylinder. (c) a portion of the lateral cross-section at point Q. Radius of the cross-section at both the ends is fixed at R_0.

sensibly assume that the deformation is symmetric with respect to the center-line or about the axis Y^3. Hence studying the deformation of one vertical line (perpendicular to the radius) between the two rigid ends is sufficient to understand the deformation behaviour of the whole cylinder. The membrane inflates outward when the gas pressure in the enclosed volume is greater than that of the surroundings i.e, when the net internal pressure is positive and inflates inward otherwise. An external magnetic field is generated along the circumferential direction by a long current carrying wire coinciding with the axis of symmetry Y^3.

We follow similar procedure as in (Reddy and Saxena, 2017) in deriving the theoretical formulation that follows.

2.2 Reference configuration

The position vector of a point in the flesh of the undeformed cylindrical membrane $\boldsymbol{X}$ is given as

$$X^1 = [R_0 + \xi] \cos \Theta, \qquad X^2 = [R_0 + \xi] \sin \Theta, \qquad X^3 = \tilde{Z}, \tag{1}$$

8

where $\boldsymbol{E}_i$ are the orthonormal basis vectors, R_0 is the radius of the initial circular cross-section and ξ is the distance of the point from the mid-surface (given by $\xi = 0$) of the membrane along the radius. Now, the bases in the curvilinear system $(\tilde{Z}, \Theta, \xi)$ at the point $\boldsymbol{X}$ become

$$\boldsymbol{G}_i = \frac{\partial \boldsymbol{X}}{\partial X^i}, \qquad \text{where } (X^1, X^2, X^3) = (\tilde{Z}, \Theta, \xi). \tag{2}$$

Components of the covariant metric tensor $G_{ij} = \boldsymbol{G}_i \cdot \boldsymbol{G}_j$ can be written as

$$G_{ij} = \begin{bmatrix} 1 & 0 & 0 \\ 0 & [R_0 + \xi]^2 & 0 \\ 0 & 0 & 1 \end{bmatrix}. \tag{3}$$

2.3 Deformed configuration

Let $\boldsymbol{p}$ denote the position of a point in the flesh of the membrane, $\boldsymbol{x}$ the position of its projection on the mid-surface along the outward normal $\boldsymbol{n}$, ξ the distance of the point from the mid-surface in reference configuration, with $\tilde{g}_{ij}$ denoting the covariant metric tensor. The relation among these quantities can be written as

$$p^i = x^i + \xi \lambda_3 n^i, \tag{4a}$$

$$\text{with} \qquad x^1 = \tilde{r}(\tilde{Z}) \cos\theta, \qquad x^2 = \tilde{r}(\tilde{Z}) \sin\theta, \qquad x^3 = \tilde{z}(\tilde{Z}). \tag{4b}$$

where the thickness stretch at the point

$$\lambda_3 = \frac{t}{T}, \tag{5}$$

with t and T representing membrane thickness at that point in deformed and reference configurations, respectively, $\tilde{r}$ representing the radial distance—from the cylinder axis Y^3—of the point which was originally at a height $\tilde{Z}$ in the reference state, $\tilde{z}$ representing the vertical distance (see Figure 1), and the azimuthal coordinate $\theta = \Theta$. These deformed coordinates can in turn be expressed in terms of the radial and axial displacements $\tilde{u}(\tilde{Z})$ and $\tilde{w}(\tilde{Z})$ respectively as

$$\tilde{r}(\tilde{Z}) = R_0 + \tilde{u}(\tilde{Z}), \qquad \theta = \Theta, \qquad \tilde{z}(\tilde{Z}) = \tilde{Z} + \tilde{w}(\tilde{Z}), \tag{6}$$

9

where all the quantities in the deformed state except the circumferential coordinate θ are functions of the axial coordinate $\tilde{Z}$. Tangent vectors at the points $\boldsymbol{x}$ and $\boldsymbol{p}$ respectively are

$$\boldsymbol{g}_i = \frac{\partial \boldsymbol{x}}{\partial X^i} \quad \text{and} \quad \tilde{\boldsymbol{g}}_i = \frac{\partial \boldsymbol{p}}{\partial X^i}, \tag{7}$$

and the components of the outward normal are

$$\boldsymbol{n} = \frac{-\boldsymbol{g}_1 \times \boldsymbol{g}_2}{|\boldsymbol{g}_1 \times \boldsymbol{g}_2|} = -\frac{1}{\sqrt{g}} \epsilon_{ijk} x^j_{,1} x^k_{,2}, \tag{8}$$

where ϵ_{ijk} is the permutation symbol and $\sqrt{g} = [R_0 + \tilde{u}]\sqrt{\tilde{u}^2_{,\tilde{Z}} + \left[1 + \tilde{w}_{,\tilde{z}}\right]^2}$ with $(\cdot)_{,\tilde{z}} = \mathrm{d}(\cdot)/\mathrm{d}\tilde{Z}$ everywhere. The negative sign here is due to the sense of $\tilde{Z}$ and Θ chosen in the problem. Expanding the above expression, we get

$$n_1 = \frac{1}{\sqrt{g}}(x^3_{,1} x^2_{,2} - x^2_{,1} x^3_{,2}) = \frac{1}{\sqrt{g}}(R_0 + \tilde{u})(1 + \tilde{w}_{,\tilde{z}})\cos\theta, \tag{9a}$$

$$n_2 = \frac{1}{\sqrt{g}}(x^1_{,1} x^3_{,2} - x^3_{,1} x^1_{,2}) = \frac{1}{\sqrt{g}}(R_0 + \tilde{u})(1 + \tilde{w}_{,\tilde{z}})\sin\theta, \tag{9b}$$

$$n_3 = \frac{1}{\sqrt{g}}(x^2_{,1} x^1_{,2} - x^1_{,1} x^2_{,2}) = \frac{-1}{\sqrt{g}}(R_0 + \tilde{u})\tilde{u}_{,\tilde{z}}. \tag{9c}$$

Components of the covariant metric tensor in the deformed state become

$$\tilde{g}_{ij} = \tilde{\boldsymbol{g}}_i \cdot \tilde{\boldsymbol{g}}_j, \quad i, j \in 1, 2, 3. \tag{10}$$

Using eqns. (4) and (8), we get

$$\tilde{g}_{ij} = \begin{bmatrix} \tilde{u}^2_{,\tilde{Z}} + \left[1 + \tilde{w}_{,\tilde{z}}\right]^2 & 0 & 0 \\ 0 & [R_0 + \tilde{u}]^2 & 0 \\ 0 & 0 & \lambda^2_3 \end{bmatrix}, \tag{11}$$

where we have neglected the thickness coordinate ξ in comparison with other dimensions. However, the derivatives with respect to the thickness coordinate ξ are not neglected. Now the

corresponding left Cauchy-Green tensor is as follows.

$$\mathbf{B} = (G_{ij})^{-1}\tilde{g}_{ij} = \begin{bmatrix} \tilde{u}^2_{,\tilde{Z}} + \left[1 + \tilde{w}_{,\tilde{Z}}\right]^2 & 0 & 0 \\ 0 & \dfrac{[R_0 + \tilde{u}]^2}{R_0^2} & 0 \\ 0 & 0 & \lambda_3^2 \end{bmatrix}. \tag{12}$$

The in-plane principal stretches λ_1 and λ_2 at a point become

$$\lambda_1 = \sqrt{\tilde{u}^2_{,\tilde{Z}} + \left[1 + \tilde{w}_{,\tilde{Z}}\right]^2}, \qquad \lambda_2 = \frac{R_0 + \tilde{u}}{R_0}. \tag{13}$$

Introducing the non-dimensional parameters

$$r = \tilde{r}/R_0, \quad u = \tilde{u}/R_0, \quad w = \tilde{w}/R_0, \quad Z = \tilde{Z}/R_0, \tag{14}$$

the principal stretches become

$$\lambda_1 = \sqrt{u'^2 + [1 + w']^2}, \qquad \lambda_2 = 1 + u, \tag{15}$$

where $(\cdot)' = \mathrm{d}(\cdot)/\mathrm{d}Z$ everywhere. We also introduce another dimensionless parameter called the aspect ratio of the cylinder for later use as

$$L_a = \frac{L}{R_0}. \tag{16}$$

3 Equations of equilibrium

3.1 Energy considerations

We take the variational formulation as presented in, for example, (Brigadnov and Dorfmann, 2003; Dorfmann and Ogden, 2003; Kankanala and Triantafyllidis, 2004) to study the weakly magnetized isotropic cylindrical membrane. As mentioned earlier, the total free energy is based on the deformation gradient (or equivalently, the principal stretches $\lambda_1, \lambda_2, \lambda_3$) and magnetization per unit mass. We refer the reader to the papers by Reddy and Saxena (2017) and Barham et al. (2007, 2008) for detailed derivations.

3.1.1 Total potential energy

The total potential energy (E) of the membrane under consideration can be written as follows.

11

$$E = T \int_{\Omega} \rho \psi \, \mathrm{d}A - T\mu_0 \int_{\Omega} \mathbf{m} \cdot \mathbf{h}_a \, \mathrm{d}A - \int_{V_0}^{V_0 + \Delta V} \tilde{P} \, \mathrm{d}V, \tag{17}$$

where ρ is the mass density, $\psi(\mathbf{F}, \boldsymbol{\mu})$ the free energy per unit mass defined in the formulation based on magnetization, T the thickness of the undeformed membrane, χ the magnetic susceptibility of the material per unit undeformed volume, $\boldsymbol{\mu}$ the material magnetization per unit mass, $\mathbf{m} = \rho\boldsymbol{\mu}$ the magnetization per unit current volume, μ_0 the permeability of free space, $\mathbf{h}_a$ the applied external magnetic field, $\tilde{P}$ the net internal pressure (difference of inside and outside pressures) and the quantity $\sqrt{G} = R_0$. Ω denotes the surface of the undeformed membrane, V_0 the enclosed initial volume and ΔV the change in this enclosed volume.

Using the following relations for a weakly magnetized membrane (self- generated magnetic field is negligible) (Barham et al., 2008),

$$\frac{\partial \psi}{\partial \boldsymbol{\mu}} = \mu_0 \mathbf{h}_a, \qquad \rho\psi(\mathbf{F}, \boldsymbol{\mu}) \approx \bar{W} + \frac{1}{2} C |\boldsymbol{\mu}|^2, \qquad C = \frac{\mu_0 \rho^2}{\chi}, \qquad \mathbf{m} = \chi \mathbf{h}_a, \tag{18}$$

and the total energy may be re-written as

$$E = \int_0^{2\pi} \int_0^L \bar{W} T \sqrt{G} \, \mathrm{d}\tilde{Z} \, \mathrm{d}\Theta - \frac{\chi}{2} \int_0^{2\pi} \int_0^L \mu_0 |\mathbf{h}_a|^2 T \sqrt{G} \, \mathrm{d}\tilde{Z} \, \mathrm{d}\Theta - \int_{V_0}^{V_0 + \Delta V} \tilde{P} \, \mathrm{d}V, \tag{19}$$

where $\bar{W}$ is the strain energy per unit undeformed volume. Let the first term, elastic strain energy be denoted by E_λ, the second term, magnetic field energy by E_h, and the third term, pressure work by E_p. Note that the strain and magnetic field energies are calculated over the reference configuration while the pressure work is over the current configuration.

3.1.2 Variation in elastic strain energy

Let the strain energy density function be expressed in terms of the principal stretches as follows

$$\bar{W}(\lambda_1, \lambda_2, \lambda_3) = \widetilde{W}\left(\tilde{u}, \frac{\mathrm{d}\tilde{u}}{\mathrm{d}\tilde{Z}}, \tilde{w}, \frac{\mathrm{d}\tilde{w}}{\mathrm{d}\tilde{Z}}\right) = W\left(u, \frac{\mathrm{d}u}{\mathrm{d}Z}, w, \frac{\mathrm{d}w}{\mathrm{d}Z}\right). \tag{20}$$

Now a variation in the strain energy density function will become

$$\delta\widetilde{W} = \frac{\partial \widetilde{W}}{\partial y^i} \delta y^i, \qquad \text{where } \left(y^1, y^2, y^3, y^4\right) = \left(\tilde{u}, \frac{\mathrm{d}\tilde{u}}{\mathrm{d}\tilde{Z}}, \tilde{w}, \frac{\mathrm{d}\tilde{w}}{\mathrm{d}\tilde{Z}}\right). \tag{21}$$

12

Note that $\mathrm{d}(\tilde{\cdot})/\mathrm{d}\tilde{Z} = \mathrm{d}(\cdot)/\mathrm{d}Z$ due to the non-dimensionalization according to eqn. (14).

Total strain energy of the membrane, E_λ can now be written as

$$E_\lambda = \int_0^{2\pi} \int_0^L \widetilde{W}\left(\tilde{u}, \frac{\mathrm{d}\tilde{u}}{\mathrm{d}\tilde{Z}}, \tilde{w}, \frac{\mathrm{d}\tilde{w}}{\mathrm{d}\tilde{Z}}\right) T\sqrt{G}\,\mathrm{d}\tilde{Z}\,\mathrm{d}\Theta = \int_0^{2\pi} \int_0^L W(u, u', w, w')\, T\sqrt{G}\,\mathrm{d}\tilde{Z}\,\mathrm{d}\Theta\ , \tag{22}$$

where the prime $(\cdot)'$ means a derivative with respect to the non-dimensional axial coordinate Z, and a variation in this energy, δE_λ is given by

$$\delta E_\lambda = \int_0^{2\pi} \int_0^{L_a} \left(\frac{\partial W}{\partial u'}\delta u' + \frac{\partial W}{\partial u}\delta u + \frac{\partial W}{\partial w'}\delta w' + \frac{\partial W}{\partial w}\delta w\right) R_0^2 T\,\mathrm{d}Z\,\mathrm{d}\Theta, \tag{23}$$

since $\tilde{Z} = R_0 Z$ and $\sqrt{G} = R_0$. We use integration by parts to convert the terms with $\delta(\cdot)'$ to those with $\delta(\cdot)$ and the boundary conditions corresponding to the fixed ends

$$u = w = 0, \quad \text{at} \quad Z = 0, L_a, \tag{24}$$

to arrive at

$$\delta E_\lambda = \int_0^{2\pi} \int_0^{L_a} \left[\left[-\frac{\mathrm{d}}{\mathrm{d}Z}\left(\frac{\partial W}{\partial u'}\right) + \frac{\partial W}{\partial u}\right]\delta u + \left[-\frac{\mathrm{d}}{\mathrm{d}Z}\left(\frac{\partial W}{\partial w'}\right) + \frac{\partial W}{\partial w}\right]\delta w\right] R_0^2 T\,\mathrm{d}Z\,\mathrm{d}\Theta. \tag{25}$$

3.1.3 Variation in pressure energy

A variation in the potential energy of the inflating gas with net internal pressure $\tilde{P}$ can be written as (Steigmann, 1990, Tielking, 1975)

$$\delta E_p = \int_0^{2\pi} \int_0^L \left[\tilde{P}\boldsymbol{n}\,\mathrm{d}a\right] \cdot \delta\boldsymbol{x}, \tag{26}$$

where $\mathrm{d}a = \sqrt{g}\,\mathrm{d}\tilde{Z}\,\mathrm{d}\Theta$ is the area of a differential element on the deformed mid-surface ($\xi = 0$) with unit normal $\boldsymbol{n}$. If the pressure surrounding the membrane is greater than that inside the membrane, numerical values of $\tilde{P}$ will be negative. Using the eqns. (4b) and (8),

$$\delta E_p = R_0^3 \int_0^{2\pi} \int_0^{L_a} \tilde{P}\left[[1 + w'][1 + u]\,\delta u - u'[1 + u]\,\delta w\right]\mathrm{d}Z\,\mathrm{d}\Theta. \tag{27}$$

13

3.1.4 Variation in energy of the magnetic field

An external magnetic field is generated by placing a current carrying wire at the axis of symmetry (Y^3 in Figure 1). The resulting magnetic field intensity $\mathbf{h}_a$ at a point in the deformed membrane can be approximated (since the thickness coordinate ξ is neglected) as

$$\mathbf{h}_a \approx \frac{I}{2\pi R_0 \left[1+u\right]}, \tag{28}$$

where I is the current in the wire and R_0 is the radius of the mid-surface of the undeformed membrane. Since the magnetic energy depends only on the radial displacement u, the variation in E_h becomes

$$\delta E_h = R_0^2 T \int_0^{2\pi} \int_0^{L_a} \frac{\chi}{2} \left[\frac{-2}{\left[1+u\right]^3} \frac{\mu_0 I^2}{4\pi^2 R_0^2}\right] \delta u \, \mathrm{d}Z \, \mathrm{d}\Theta. \tag{29}$$

3.2 Elastic constitutive models

We study four constitutive models namely neo-Hookean, Mooney-Rivlin, Ogden and Aruda-Boyce for the elastic strain energy density $\bar{W}$ in eqn. $(18)_2$ and further assume the material to be incompressible ($\lambda_1 \lambda_2 \lambda_3 = 1$). Thus we have

$$\widehat{W}(\lambda_1, \lambda_2) = \bar{W}\left(\lambda_1, \lambda_2, \frac{1}{\lambda_1 \lambda_2}\right). \tag{30}$$

3.2.1 Ogden model

The strain energy density proposed by Ogden (1972) to model nonlinear elastic solids can be written as

$$\widehat{W} = \sum_{k=1}^{K} \frac{\mu_k}{\alpha_k} \left[\lambda_1^{\alpha_k} + \lambda_2^{\alpha_k} + \left[\frac{1}{\lambda_1 \lambda_2}\right]^{\alpha_k} - 3\right], \tag{31}$$

with the conditions $\sum_k \mu_k \alpha_k = 2\mu$ and $\mu_k \alpha_k > 0$. Choosing $K = 3$, we define the following non-dimensional parameters

$$\mu_1^* = \mu_1/\mu, \qquad \mu_2^* = \mu_2/\mu, \qquad \mu_3^* = \mu_3/\mu, \tag{32}$$

maintaining $\sum_k \mu_k \alpha_k = 2\mu$ with $\mu = 0.4145$ MPa for our numerical analysis.

14

3.2.2 Neo-Hookean

Substituting $k = 1$, $\mu_1 = \mu$, and $\alpha_1 = 2$ in the expression for the Ogden strain energy density (eqn. (31)), we obtain the expression for neo-Hookean energy as

$$\widehat{W} = \frac{\mu}{2} \left[\lambda_1^2 + \lambda_2^2 + \left[\frac{1}{\lambda_1 \lambda_2} \right]^2 - 3 \right]. \tag{33}$$

3.2.3 Mooney-Rivlin

Substituting $k = \{1, 2\}$, $\alpha_1 = 2$ and $\alpha_2 = -2$ in the expression for the Ogden strain energy density (eqn. (31)), we obtain the expression for Mooney-Rivlin energy as

$$\widehat{W} = \frac{\mu_1}{2} \left[\lambda_1^2 + \lambda_2^2 + \left[\frac{1}{\lambda_1 \lambda_2} \right]^2 - 3 \right] - \frac{\mu_2}{2} \left[\lambda_1^{-2} + \lambda_2^{-2} + \left[\frac{1}{\lambda_1 \lambda_2} \right]^{-2} - 3 \right]. \tag{34}$$

We use the following non-dimensional parameters

$$\mu_1^* = \mu_1/\mu, \qquad \mu_2^* = \mu_2/\mu, \tag{35}$$

maintaining $\sum_k \mu_k \alpha_k = 2\mu$ for our numerical analysis.

3.2.4 Arruda-Boyce (eight chain model)

The original constitutive model proposed by Arruda and Boyce (1993) involves an inverse Langevin function which does not have an explicit form. Hence, many approximations for this function have been developed. Jedynak (2015) presents a review and comparison of such approximations available in the literature. Here we use a series expansion mentioned in Treloar (1954), Arruda and Boyce (1993, eqn. (21)), Boyce and Arruda (2000, eqn. (26)) and Steinmann et al. (2012),

$$\widehat{W} = \mu \sum_{k=1}^{K} \frac{c_k}{N^{k-1}} \left[I_1^k - 3^k \right], \tag{36}$$

where

$$I_1 = \lambda_1^2 + \lambda_2^2 + \left[\frac{1}{\lambda_1 \lambda_2} \right]^2 \tag{37}$$

is the first invariant of the left Cauchy-Green tensor, μ is shear modulus and N stands for the number of Kuhn segments.

15

3.3 Governing Equations

According to the principle of minimum potential energy, equilibrium is obtained when

$$\delta E = \delta E_\lambda - \delta E_h - \delta E_p = 0, \tag{38}$$

that results in the following equations.

$$\frac{\partial W}{\partial u} - \frac{\mathrm{d}}{\mathrm{d}Z}\left(\frac{\partial W}{\partial u'}\right) + \frac{\chi \mu_0 I^2}{4\pi^2 R_0^2 \left[1 + u\right]^3} - \frac{\tilde{P} R_0}{T}\left[1 + w'\right]\left[1 + u\right] = 0, \tag{39a}$$

$$\frac{\partial W}{\partial w} - \frac{\mathrm{d}}{\mathrm{d}Z}\left(\frac{\partial W}{\partial w'}\right) + \frac{\tilde{P} R_0}{T} u'\left[1 + u\right] = 0. \tag{39b}$$

From eqn. (20), the partial derivatives of W can be written as

$$\frac{\partial W}{\partial u'} = \frac{\partial \widehat{W}}{\partial \lambda_1}\frac{\partial \lambda_1}{\partial u'} + \frac{\partial \widehat{W}}{\partial \lambda_2}\frac{\partial \lambda_2}{\partial u'}, \tag{40a}$$

$$\frac{\partial W}{\partial w'} = \frac{\partial \widehat{W}}{\partial \lambda_1}\frac{\partial \lambda_1}{\partial w'} + \frac{\partial \widehat{W}}{\partial \lambda_2}\frac{\partial \lambda_2}{\partial w'}, \tag{40b}$$

$$\frac{\partial W}{\partial u} = \frac{\partial \widehat{W}}{\partial \lambda_1}\frac{\partial \lambda_1}{\partial u} + \frac{\partial \widehat{W}}{\partial \lambda_2}\frac{\partial \lambda_2}{\partial u}, \tag{40c}$$

$$\frac{\partial W}{\partial w} = \frac{\partial \widehat{W}}{\partial \lambda_1}\frac{\partial \lambda_1}{\partial w} + \frac{\partial \widehat{W}}{\partial \lambda_2}\frac{\partial \lambda_2}{\partial w}. \tag{40d}$$

Using the partial derivatives of the principal stretches evident from eqn. (15),

$$\frac{\partial \lambda_1}{\partial u'} = \frac{u'}{\lambda_1}, \quad \frac{\partial \lambda_2}{\partial u'} = 0, \quad \frac{\partial \lambda_1}{\partial w'} = \frac{1 + w'}{\lambda_1}, \quad \frac{\partial \lambda_2}{\partial w'} = 0, \tag{41a}$$

$$\frac{\partial^2 \lambda_1}{\partial u' \partial u'} = \frac{\left[1 + w'\right]^2}{\lambda_1^3}, \quad \frac{\partial^2 \lambda_1}{\partial w' \partial w'} = \frac{u'^2}{\lambda_1^3}, \quad \frac{\partial^2 \lambda_1}{\partial w' \partial u'} = \frac{\partial^2 \lambda_1}{\partial u' \partial w'} = -\frac{u'\left[1 + w'\right]}{\lambda_1^3}, \tag{41b}$$

$$\frac{\partial \lambda_1}{\partial u} = 0, \quad \frac{\partial \lambda_2}{\partial u} = 1, \quad \frac{\partial \lambda_1}{\partial w} = 0, \quad \frac{\partial \lambda_2}{\partial w} = 0, \tag{41c}$$

$$\lambda_1' = \frac{u'u'' + \left[1 + w'\right]w''}{\lambda_1}, \quad \lambda_2' = u', \tag{41d}$$

the relations (40) become

$$\frac{\partial W}{\partial u'} = \frac{\partial \widehat{W}}{\partial \lambda_1}\left[\frac{u'}{\lambda_1}\right], \qquad \frac{\partial W}{\partial w'} = \frac{\partial \widehat{W}}{\partial \lambda_1}\left[\frac{1 + w'}{\lambda_1}\right], \qquad \frac{\partial W}{\partial u} = \frac{\partial \widehat{W}}{\partial \lambda_2}, \qquad \frac{\partial W}{\partial w} = 0. \tag{42}$$

16

The governing equations (39) can then be written from the relations (42) as

$$\frac{\partial \widehat{W}}{\partial \lambda_2} - \frac{u'}{\lambda_1}\frac{\mathrm{d}}{\mathrm{d}Z}\left(\frac{\partial \widehat{W}}{\partial \lambda_1}\right) - \frac{\partial \widehat{W}}{\partial \lambda_1}\frac{\mathrm{d}}{\mathrm{d}Z}\left(\frac{u'}{\lambda_1}\right) + \frac{\chi \mu_0 I^2}{4\pi^2 R_0^2[1+u]^3} - \frac{\tilde{P}R_0}{T}\left[1+u\right]\left[1+w'\right] = 0, \quad (43a)$$

$$\frac{1+w'}{\lambda_1}\frac{\mathrm{d}}{\mathrm{d}Z}\left(\frac{\partial \widehat{W}}{\partial \lambda_1}\right) + \frac{\partial \widehat{W}}{\partial \lambda_1}\frac{\mathrm{d}}{\mathrm{d}Z}\left(\frac{1+w'}{\lambda_1}\right) - \frac{\tilde{P}R_0}{T}\left[1+u\right]u' = 0. \quad (43b)$$

Defining the magnetic energy parameter in terms of shear modulus μ appearing in the previous section as

$$\mathcal{M} = \frac{\mu_0 I^2}{4\pi^2 R_0^2 \mu}, \quad (44)$$

and a non-dimensional pressure as

$$P = \frac{\tilde{P}R_0}{\mu T}, \quad (45)$$

we arrive at the following useful form of the governing equations.

$$\frac{1}{\mu}\frac{\partial \widehat{W}}{\partial \lambda_2} - \frac{1}{\mu}\frac{u'}{\lambda_1}\frac{\mathrm{d}}{\mathrm{d}Z}\left(\frac{\partial \widehat{W}}{\partial \lambda_1}\right) - \frac{1}{\mu}\frac{\partial \widehat{W}}{\partial \lambda_1}\frac{\mathrm{d}}{\mathrm{d}Z}\left(\frac{u'}{\lambda_1}\right) + \frac{\chi \mathcal{M}}{[1+u]^3} - P[1+u][1+w'] = 0, \quad (46a)$$

$$\frac{1}{\mu}\frac{1+w'}{\lambda_1}\frac{\mathrm{d}}{\mathrm{d}Z}\left(\frac{\partial \widehat{W}}{\partial \lambda_1}\right) + \frac{1}{\mu}\frac{\partial \widehat{W}}{\partial \lambda_1}\frac{\mathrm{d}}{\mathrm{d}Z}\left(\frac{1+w'}{\lambda_1}\right) - P[1+u]u' = 0. \quad (46b)$$

3.3.1 Stability of equilibrium

A necessary condition for the equilibrium state obtained from solution of the governing equations (46) to be a minimizer of the energy functional (19) is that the second variation be positive that results in the conditions that the matrix

$$\mathbf{P} = \frac{1}{2}\begin{bmatrix} \mathcal{F}_{u'u'} & \mathcal{F}_{u'w'} \\ \mathcal{F}_{w'u'} & \mathcal{F}_{w'w'} \end{bmatrix}, \quad (47)$$

with

$$\mathcal{F} = \widehat{W}\,TR_0^2 - \frac{\chi}{2}\mu_0|\mathbf{h}_a|^2 TR_0^2 - \frac{1}{2}\tilde{P}R_0^3\left[1+u\right]^2\left[1+w'\right], \quad (48)$$

being the integrand in eqn. (19) be positive definite for all $Z \in [0, L_a]$. A simple but rather restrictive sufficient condition for minimization (Gelfand and Fomin, 2000, Ch. 5) is that a non-zero solution to the following differential equation exists and is invertible for all $Z \in [0, L_a]$

$$-\frac{\mathrm{d}}{\mathrm{d}Z}(\mathbf{P}\mathbf{U}') + \mathbf{Q}\mathbf{U} = 0, \qquad \mathbf{U}(0) = \begin{bmatrix} 0 & 0 \\ 0 & 0 \end{bmatrix}, \quad \mathbf{U}'(0) = \begin{bmatrix} 1 & 0 \\ 0 & 1 \end{bmatrix}, \quad (49)$$

where

$$\mathbf{Q} = \frac{1}{2} \begin{bmatrix} \mathcal{F}_{uu} & \mathcal{F}_{uw} \\ \mathcal{F}_{wu} & \mathcal{F}_{ww} \end{bmatrix} - \frac{1}{2} \frac{\mathrm{d}}{\mathrm{d}Z} \left(\begin{bmatrix} \mathcal{F}_{uu'} & \mathcal{F}_{uw'} \\ \mathcal{F}_{wu'} & \mathcal{F}_{ww'} \end{bmatrix} \right). \tag{50}$$

Since the sufficient condition is strong, we get certain cases where only the necessary condition is met and we are unable to comment on the stability of the equilibrium state.

If

$$\mathbf{P} = \frac{1}{2} \begin{bmatrix} P_1 & P_2 \\ P_3 & P_4 \end{bmatrix}, \quad \mathbf{Q} = \frac{1}{2} \begin{bmatrix} Q_1 & Q_2 \\ Q_3 & Q_4 \end{bmatrix}, \quad \mathbf{U} = \begin{bmatrix} U_1 & U_2 \\ U_3 & U_4 \end{bmatrix}, \tag{51a}$$

$$\{U_1, U_1', U_2, U_2', U_3, U_3', U_4, U_4'\} = \{u_1, u_2, u_3, u_4, u_5, u_6, u_7, u_8\}, \tag{51b}$$

the sufficient condition (49) can be written as

$$\begin{bmatrix} 1 & 0 & 0 & 0 & 0 & 0 & 0 & 0 \\ 0 & -P_1 & 0 & 0 & 0 & -P_2 & 0 & 0 \\ 0 & 0 & 1 & 0 & 0 & 0 & 0 & 0 \\ 0 & 0 & 0 & -P_1 & 0 & 0 & 0 & -P_2 \\ 0 & 0 & 0 & 0 & 1 & 0 & 0 & 0 \\ 0 & -P_3 & 0 & 0 & 0 & -P_4 & 0 & 0 \\ 0 & 0 & 0 & 0 & 0 & 0 & 1 & 0 \\ 0 & 0 & 0 & -P_3 & 0 & 0 & 0 & -P_4 \end{bmatrix} \begin{bmatrix} u_1' \\ u_2' \\ u_3' \\ u_4' \\ u_5' \\ u_6' \\ u_7' \\ u_8' \end{bmatrix} = \begin{bmatrix} u_2 \\ P_1'u_2 + P_2'u_6 - Q_1 u_1 - Q_2 u_5 \\ u_4 \\ P_1'u_4 + P_2'u_8 - Q_1 u_3 - Q_2 u_7 \\ u_6 \\ P_3'u_2 + P_4'u_6 - Q_3 u_1 - Q_4 u_5 \\ u_8 \\ P_3'u_4 + P_4'u_8 - Q_3 u_3 - Q_4 u_7 \end{bmatrix}, \quad \begin{bmatrix} u_1' \\ u_2' \\ u_3' \\ u_4' \\ u_5' \\ u_6' \\ u_7' \\ u_8' \end{bmatrix}_{Z=0} = \begin{bmatrix} 0 \\ 1 \\ 0 \\ 0 \\ 0 \\ 0 \\ 0 \\ 1 \end{bmatrix}.$$
$$\tag{52}$$

The expressions for the elements of matrices $\mathbf{P}$ and $\mathbf{Q}$ can be found in the appendix A.

3.3.2 Relaxed strain energy density

Since membranes are no-compression structures, a modification in the strain energy density function is required to account for wrinkling. The cylindrical membrane under consideration can have mechanical compression only in the circumferential direction Θ, hence the circumferential stretch λ_2 can be replaced by a function of the meridional stretch λ_1 as explained below (Pipkin, 1986). Note that this modification is required only in the expression for elastic energy E_λ (see eqn. (22)) while the deformation parameters (u, u', w, w') in the expressions for magnetic energy E_h (eqn. (29)) and pressure work E_p (eqn. (26)) should be left as they are. A zero mechanical

stress along the Θ direction implies

$$\frac{\partial \widehat{W}}{\partial \lambda_2} = 0. \tag{53}$$

From Sec. 3.2, for all the four constitutive models, the above equation gives

$$\lambda_2 = \frac{1}{\sqrt{\lambda_1}}. \tag{54}$$

Now the relaxed strain energy density for incompressible materials ($\lambda_1 \lambda_2 \lambda_3 = 1$) becomes (see Sec. 3.2)

$$\text{Ogden:} \qquad \widehat{W}_r(\lambda_1) = \sum_{k=1}^{K} \frac{\mu_k}{\alpha_k} \left[\lambda_1^{\alpha_k} + 2\lambda_1^{-\alpha_k/2} - 3 \right], \tag{55}$$

$$\text{neo-Hookean:} \qquad \widehat{W}_r(\lambda_1) = \frac{\mu}{2} \left[\lambda_1^2 + \frac{2}{\lambda_1} - 3 \right], \tag{56}$$

$$\text{Mooney-Rivlin:} \qquad \widehat{W}_r(\lambda_1) = \frac{\mu_1}{2} \left[\lambda_1^2 + \frac{2}{\lambda_1} - 3 \right] - \frac{\mu_2}{2} \left[\lambda_1^{-2} + 2\lambda_1 - 3 \right], \tag{57}$$

$$\text{Arruda-Boyce:} \qquad \widehat{W}_r(\lambda_1) = \mu \sum_{k=1}^{K} \frac{c_k}{N^{k-1}} \left[I_1^k - 3^k \right], \quad \text{with} \quad I_1 = \lambda_1^2 + \frac{2}{\lambda_1}. \tag{58}$$

The corresponding governing equations can be obtained from eqns. (46) by replacing the strain energy density, $\widehat{W}$ by relaxed energy density $\widehat{W}_r$ and putting the derivative of $\widehat{W}$ with respect to the circumferential stretch λ_2 to zero.

4 Numerical Procedure

The coupled second order governing ODEs (46) with the boundary conditions (24) are solved numerically using a finite difference method coupled with a cubic extrapolation arc-length technique as laid out in (Patil et al., 2015b).

A vertical edge of the cylinder from $Z = 0$ to $Z = L_a$ is discretized into $\mathcal{N}$ uniformly distributed grids (of length $\Delta Z = L_a/\mathcal{N}$) thereby producing $\mathcal{N} + 1$ nodes. Derivatives (u', w') of the degrees of freedom (u, w) are approximated by central differences at every node except

the ends. Forward and backward differences are used at the ends as shown below

$$u_1' = \frac{u_2 - u_1}{\Delta Z}, \quad w_1' = \frac{w_2 - w_1}{\Delta Z}, \tag{59a}$$

$$u_{\mathcal{N}+1}' = \frac{u_{\mathcal{N}+1} - u_{\mathcal{N}}}{\Delta Z}, \quad w_{\mathcal{N}+1}' = \frac{w_{\mathcal{N}+1} - w_{\mathcal{N}}}{\Delta Z}, \tag{59b}$$

$$u_i' = \frac{u_{i+1} - u_{i-1}}{2\Delta Z}, \quad w_i' = \frac{w_{i+1} - w_{i-1}}{2\Delta Z}, \tag{59c}$$

$$u_i'' = \frac{u_{i+1} - 2u_i + u_{i-1}}{\Delta Z^2}, \quad w_i'' = \frac{w_{i+1} - 2w_i + w_{i-1}}{\Delta Z^2}, \quad i = 2 \text{ to } \mathcal{N}. \tag{59d}$$

In an iteration, whether to use the relaxed strain energy density at a node i is determined by the initial guess available to that iteration. Principal stretches

$$\lambda_{1i} = \sqrt{u_i'^2 + [1 + w_i']^2}, \quad \lambda_{2i} = 1 + u_i, \tag{60}$$

at every node are evaluated according to the discretization scheme described earlier and the condition for impending wrinkling

$$\lambda_{2i}^2 \lambda_{1i} \leq 1, \tag{61}$$

is checked for.

Now the governing equations (46) at internal nodes ($i = 2$ to $\mathcal{N}$) lead to $2[\mathcal{N} - 1]$ algebraic equations

$$f_{1i}(u_{i-1}, w_{i-1}, u_i, w_i, u_{i+1}, w_{i+1}) = 0, \tag{62a}$$

$$f_{2i}(u_{i-1}, w_{i-1}, u_i, w_i, u_{i+1}, w_{i+1}) = 0, \tag{62b}$$

and the boundary conditions (24) become

$$u_1 = w_1 = u_{\mathcal{N}+1} = w_{\mathcal{N}+1} = 0. \tag{63}$$

The set of nonlinear algebraic equations (62) are solved in the commercially available software MATLAB$^{\circledR}$ 2016a using the inbuilt function `fsolve`. Search for a solution is stopped when the norm of the vector containing the left-hand-sides of the algebraic equations (62) becomes lower than 10^{-10}. This method is, however, sensitive to the initial guess provided and many manual trials may be required before arriving at a solution. Often, solutions obtained previously for a different set of parameters like P or $\mathcal{M}$ were used as initial guesses if a similar deformed shape of the membrane is expected.

Initial guess, for an iteration k, of the loading parameter P and degrees of freedom u_i, w_i ($i = 2$ to $\mathcal{N}$) is evaluated using a cubic extrapolation arc-length technique mentioned in Patil et al. (2015b). For example, solution

$$s_k = \begin{bmatrix} P^k & u_1^k & w_1^k & \cdots & u_i^k & w_i^k & \cdots & u_{\mathcal{N}+1}^k & w_{\mathcal{N}+1} \end{bmatrix}, \tag{64}$$

from the previous four iterations (s_0, s_1, s_2, s_3) are used to evaluate the initial guess for the next iteration (s_4) as follows.

$$s_4 = \sum_{a=0}^{a=3} \left[\prod_{b=0, b\neq a}^{b=3} \frac{l_4 - l_b}{l_a - l_b} \right] s_a, \tag{65}$$

where l is an arc-length function taking the following values for the previous iterations.

$$l_0 = 0, \ \ l_1 = ||s_1 - s_0||, \ \ l_2 = l_1 + ||s_2 - s_1||, \ \ l_3 = l_2 + ||s_3 - s_2||, \tag{66a}$$

$$l_4 = l_3 + ||s_3 - s_2||, \tag{66b}$$

with $|| \cdot ||$ representing the usual Euclidean norm of the vector.

The above procedure can be used to trace the pressure-stretch plots at a given magnetic loading $\mathcal{M}$. The first four equilibrium states, however, need to be obtained manually by trial and error. In this study, equilibrium states were found easily at relatively small values of internal or external pressure with the initial guess $u_i = w_i = 0$ at all the $\mathcal{N} + 1$ nodes.

5 Numerical results

Table 1: Dimensionless parameters used in the computations

Mooney-Rivlin (Arruda and Boyce, 1993, Appendix)					
μ_1^*			μ_2^*		
0.9091			-0.09091		
Ogden (Ogden, 1972)					
μ_1^*	μ_2^*	μ_3^*	α_1	α_2	α_3
1.4910	0.0029	-0.0236	1.3	5.0	-2.0
Arruda-Boyce (Arruda and Boyce, 1993, eqn. (21))					
c_1	c_2	c_3	c_4	c_5	N
1/2	1/20	11/1050	19/7000	519/673750	26.5
χ					
2.5					

21

$L_a = 6, \mu_1^* = 2.0, \mu_2^* = -0.2, \mathcal{M} = 0$

(a)

$L_a = 6, \mu_1^* = 2.0, \mu_2^* = -0.2, \mathcal{M} = 0$

(b)

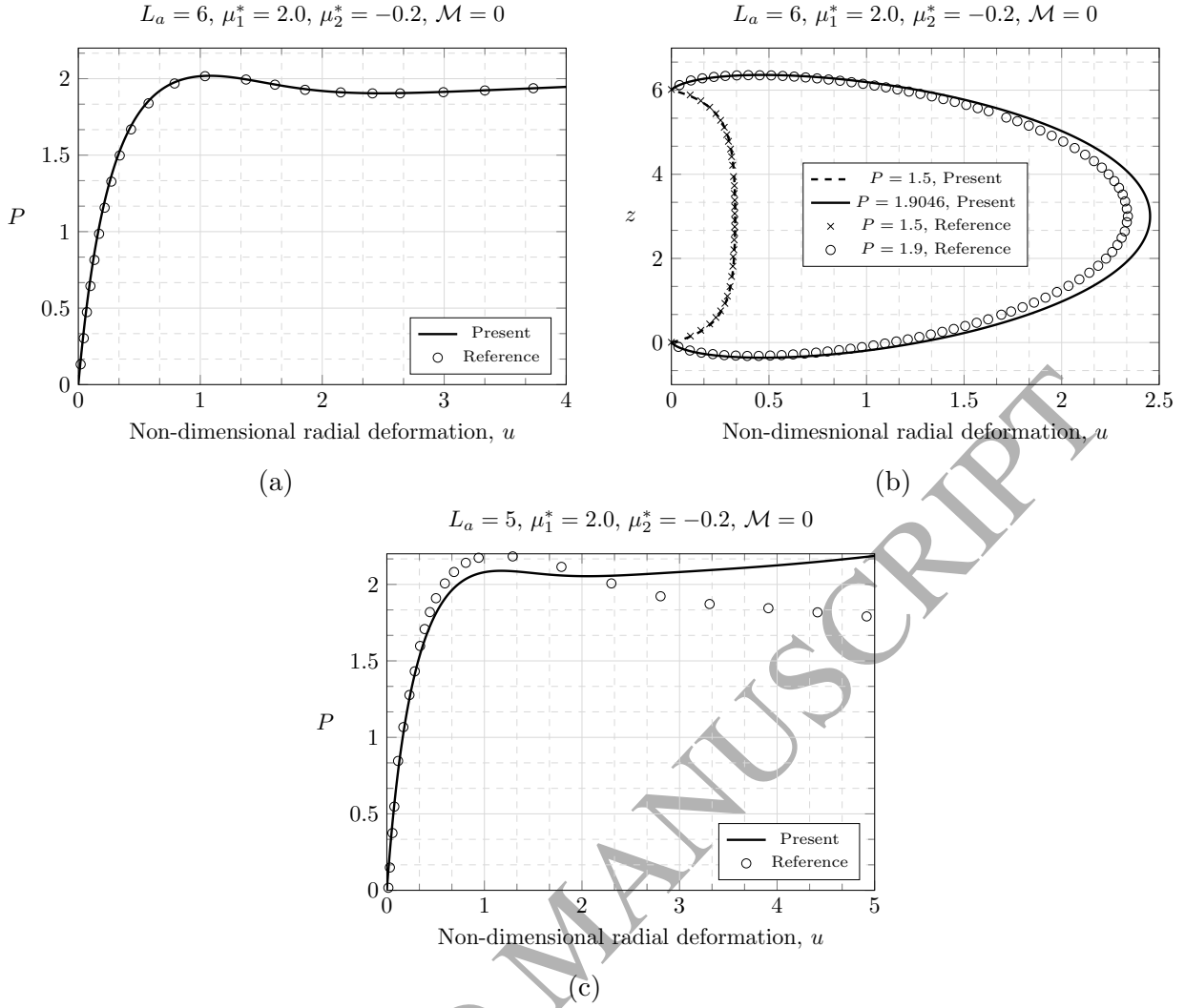$L_a = 5, \mu_1^* = 2.0, \mu_2^* = -0.2, \mathcal{M} = 0$

(c)

Figure 2: Comparison of our numerical solutions with (a), (b) Patil et al. (2014) and (c) Khayat et al. (1993) for purely mechanical deformation.

5.1 Validating the formulation

An agreeable matching of our present results with those of Patil et al. (2014) for a purely elastic case in Figure 2a and Figure 2b demonstrates the authenticity of the numerical implementation of the formulation presented in the earlier sections. A similar variational approach described here in this article is used in Patil et al. (2014) while a direct force balance approach is taken by Khayat et al. (1993). This difference in our approaches may be the reason for the disparity observed in Figure 2c.

5.1.1 Comparison of the constitutive models

While many researchers did study the behaviour of various constitutive models of elasticity separately, a direct comparison of the four models specified in section 3.2 is not available in the literature. Also, Arruda-Boyce model has not been previously used to study cylindrical
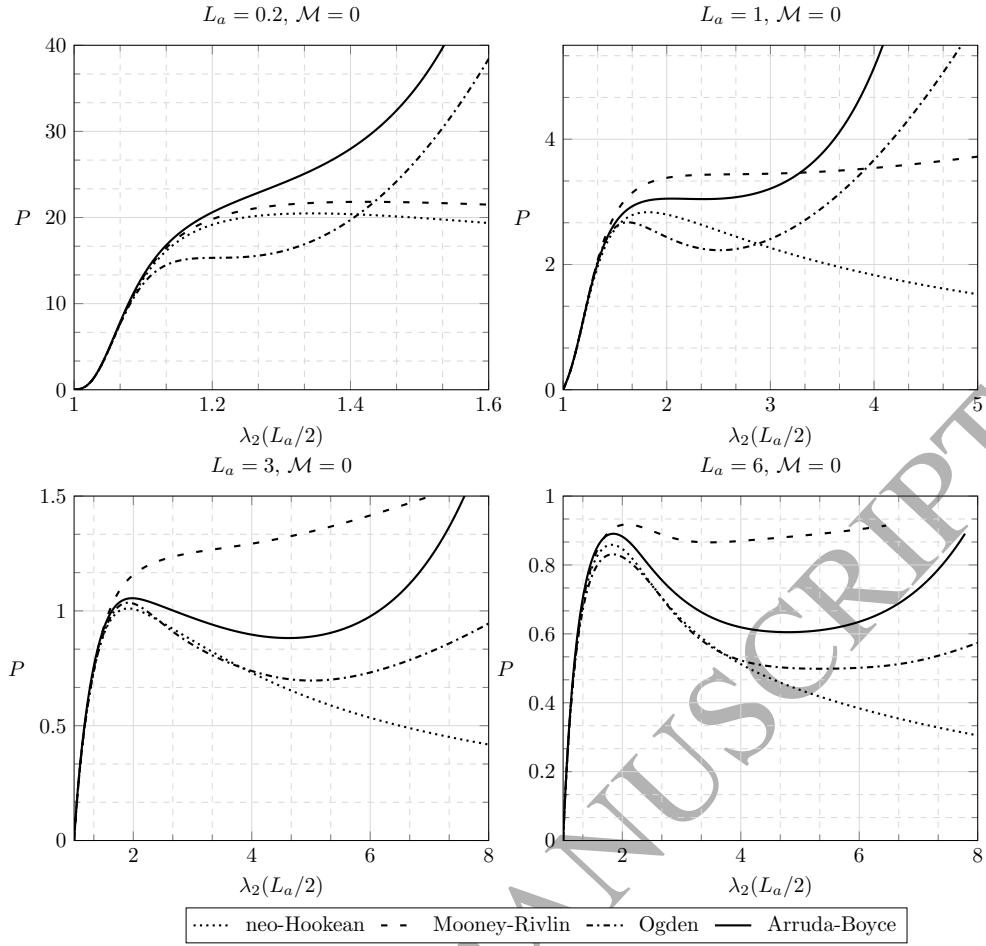
22

Figure 3: Comparison of the various constitutive models for a purely elastic case for the parameters chosen.

membranes or the bulging instability. A comparison of the many constitutive models in this context can be a separate study in itself. While this comparison is not the primary objective of this study, we take this opportunity to present a few findings of our own.

It is first required to evaluate the various parameters involved in the strain energy functions–c_k, N, α_k, μ_k–using experimental data before proceeding further with theoretical analysis. We use the numerical values from the available studies on bulk materials and are presented in Table 1.

Figure 3 shows a comparison of the models in case of purely elastic cylinders of various aspect ratios. Only the variation of the circumferential stretch at the mid-length $Z = L_a/2$ with the inflating pressure is shown. Mooney-Rivlin model seems to estimate the maximum value for elastic limit point pressure where it is possible and the minimum value by neo-Hookean (bottom left, Figure 3) or Ogden models (top left, top right, bottom right, Figure 3). No
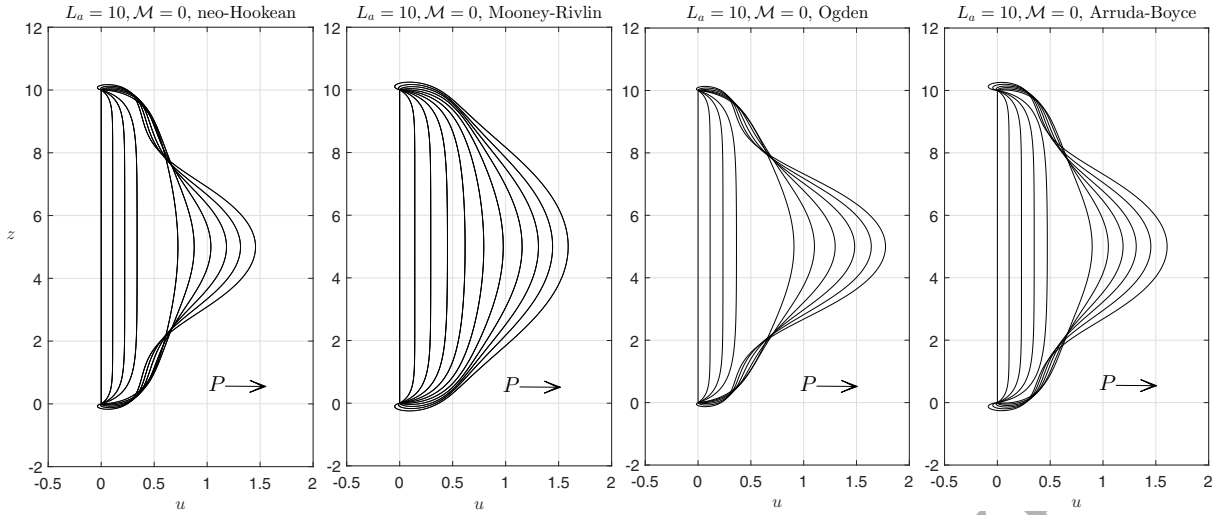
Figure 4: Depiction of bulging instability in a long cylinder with an aspect ratio $L_a = 10$. Various curves represent the deformed axisymmetric profiles of the membrane. Arrows indicate the direction of increase in internal pressure. All the models except Mooney-Rivlin predict this phenomenon although the pressures at which it starts may differ.

stationary points are predicted by some models for lower aspect ratios of the cylinder. For example, Arruda-Boyce model doesn't predict for $L_a = 0.2$ and Mooney-Rivlin doesn't seem to predict for cylinders with $L_a \leq 3$.

All the four models give almost identical results at lower pressures, typically below the limit point pressure. Post this point, pressure-stretch curves corresponding to the Ogden and Arruda-Boyce models have similar shapes while significantly deviating from those corresponding to neo-Hookean or Mooney-Rivlin models. Also, the curves given by neo-Hookean and Mooney-Rivlin models seem to get farther from each other upon increasing the aspect ratio L_a.

The onset of strain-hardening happens the earliest in a Mooney-Rivlin material while neo-Hookean can not predict this at all. While the pressure required for inflation just after the elastic limit point is overestimated by Mooney-rivlin model, pressure required late after the limit point is the maximum in an Arruda-Boyce material. There is a huge disparity in all four models at large values of λ_2.

Figure 4 shows a few deformed profiles of a purely elastic cylinder of aspect ratio $L_a = 10$. While it is a known fact that neo-Hookean and Ogden models do predict the bulging instability (Skala, 1970; Kyriakides and Yu-Chung, 1991), the 2-parameter Mooney-Rivlin model does not (Skala, 1970). Now, it can be seen from Figure 4 that Arruda-Boyce model also can predict this phenomenon.

24

5.2 Outward inflation

Figure 5 shows the behaviour of the membrane in the presence of an external magnetic field due to a current carrying wire held stationary at the axis of symmetry. The behaviour observed here is similar to that observed by us (Reddy and Saxena, 2017) for a magnetoelastic toroidal membrane. It is evident from Figure 5 that more internal pressure is required to inflate the membrane to a given stretch in the presence of a magnetic field since the magnetic field shrinks the material–the ferromagnetic particles inside attract each other. By extension, the traditional elastic limit point pressure increases with increasing current in the wire or equivalently, $\mathcal{M}$ (see figures 5b, 5c).

It can also be noticed that the pressure-stretch plots corresponding to non-zero values of the magnetic energy parameter $\mathcal{M}$ do not start at zero pressure P. A certain amount of internal pressure is required to overcome the compression caused by the magnetic field and initiate the inflation process. What happens to the left of the starting points of these curves is elaborated in section 5.3.1.

For certain values of $\mathcal{M}$, an initial dip in the internal pressure can be seen in figures 5b-5e. This fall in pressure begins upon overcoming the 'magnetic stiffness' until the elastic stiffness gains dominance. After this point, the behaviour is same as that of a purely elastic membrane. More pressure is required after this to inflate the membrane until pressure work overcomes the elastic stiffness at the traditional elastic limit point as in Figure 5c. Beyond a certain value of $\mathcal{M}$, the traditional elastic limit point vanishes and the pressure required for inflation P reduces monotonously. An analogous behaviour can be seen where the elastic limit point is not present. For example, for $\mathcal{M} = 18.0$ in Figure 5a, pressure decreases continuously until the behaviour is same as that for other values of $\mathcal{M}$.

In this case, inflation starts once the amount of pressure overcomes both the magnetic and elastic stiffnesses right at the beginning of the inflation process. Contrary to other cylinders, the short cylinder of aspect ratio $L_a = 0.2$ does not show initial fall in internal pressure P. It may be argued that elastic stiffness is dominant from the very beginning of the inflation process. The fact that the magnetic field intensity $|\boldsymbol{h}_a|$ reduces with the distance (see eqn. (28)) means the effect of the current carrying wire is nullified at larger stretches resulting in the convergence of all curves as seen in the Figure 5.
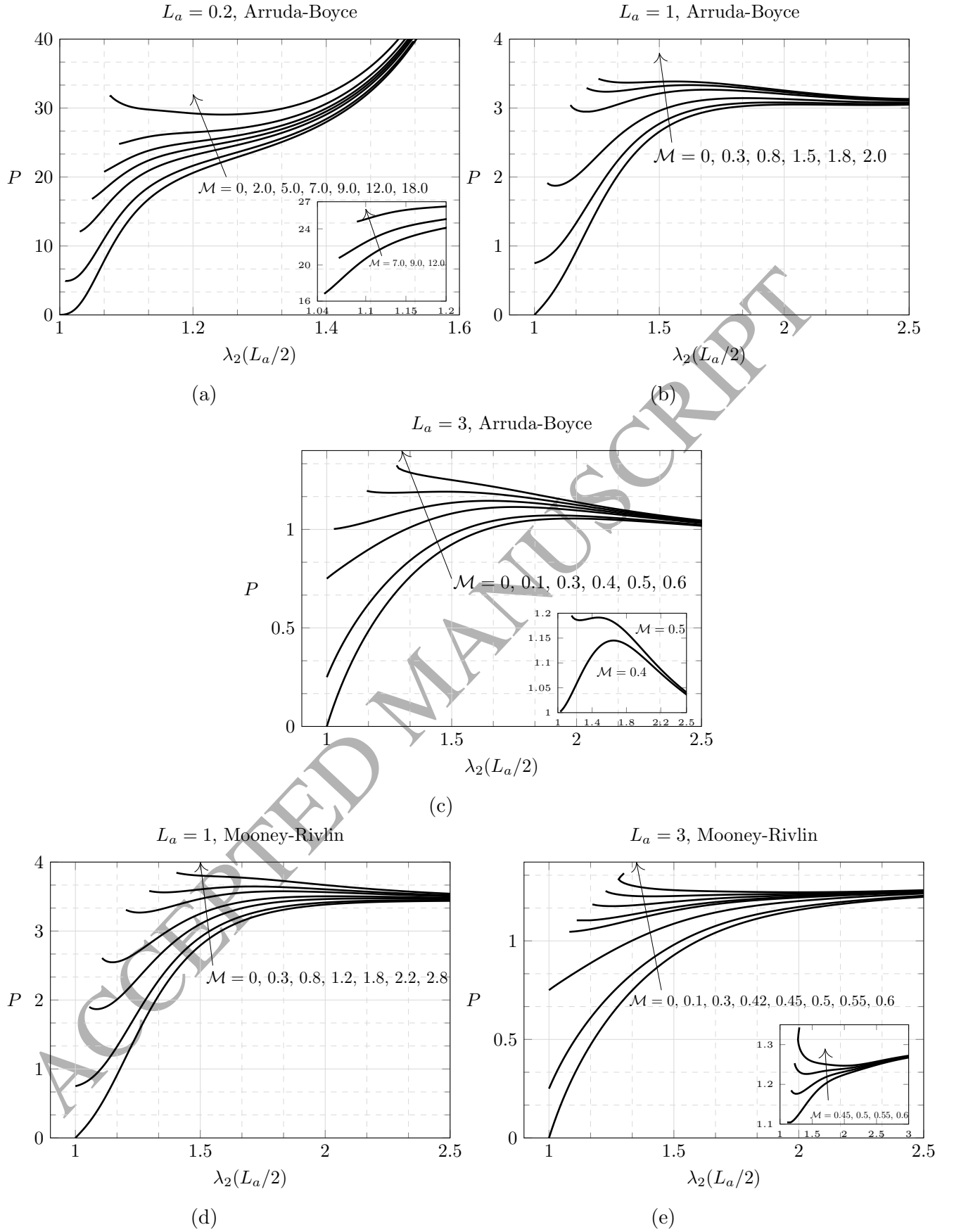
25

Figure 5: Effect of the external magnetic field on the outward inflation. All the models predict the same behaviour. Only the results for (a), (b), (c) Arruda-Boyce (with $N = 26.5$) and (d),(e) Mooney-Rivlin models are shown here. Small portions of the plot areas are magnified in inset figures in (a), (c) and (e) for better visualization.

26

Figures 5b-5e also show that strengthening the external magnetic field (or increasing $\mathcal{M}$) shifts the first stationary point (local minimum) to greater stretches and the second stationary point (local maximum) to lower stretches. These two extrema merge at a particular value of magnetic energy parameter $\mathcal{M}$ as is apparent in Figure 5c. Above this value of $\mathcal{M}$, a monotonous decrease in inflating pressure P will be seen at the beginning. This behaviour is true for other cylinders that exhibit two stationary points.

It can also be noticed that with increase in the aspect ratio L_a of the cylinder, the presence of the initial fall in gas pressure becomes less and less apparent and that smaller values of $\mathcal{M}$ can lead to the said behaviour. This is expected since reducing the initial radius of the cylinder, R_0 at a fixed length L brings the membrane closer to the current carrying wire thereby increasing the magnetic energy in it.

A note on the stability of the equilibrium states: in a few instances where initial fall in the internal pressure can be seen (for example, the curve corresponding to $\mathcal{M} = 0.8$ in Figure 5b), a few solutions at the beginning of the curve are found not to satisfy the sufficient condition of stability criterion described in Sec. 3.3.1. Hence their stability remains undetermined according to the scheme proposed. Nevertheless, eliminating these equilibrium states does not change the membrane behaviour observed. We (Reddy and Saxena, 2017) also had similar pressure-stretch curves for a toroidal magnetoelastic membrane with all stable states. Extending this observation, the current equilibrium states may be considered stable.

5.3 Inward inflation

Figure 6 shows the pressure-stretch plots for purely elastic cylinders of various aspect ratios and for all the four constitutive models. Negative net internal pressure means that the external pressure is greater than the internal pressure. Compared to outward inflation, smaller pressures can induce a given strain. Also, deforming inward a cylinder of larger aspect ratio requires less pressure than deforming one with a smaller aspect ratio just as bending a longer cantilever beam is simpler. Contrary to the results observed during outward inflation, all the four constitutive models seem to produce very close results as is evident from Figure 6. Hence the results for a neo-Hookean material only will be discussed further.
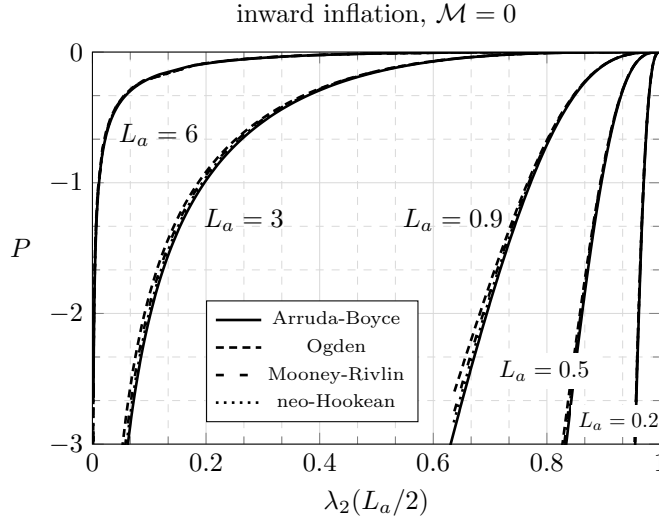
27

Figure 6: Variation of the circumferential stretches at mid-length ($Z = L_a/2$) with the dimensionless external pressure for various aspect ratios (mentioned on or adjacent to the curves). Negative sign means vacuum within the volume enclosed by the membrane. Contrary to the outward inflation, small values of pressure can lead to enormous amounts of strain in inward inflation.

Figure 7 shows a typical behaviour of the membrane under inward inflation. Only a few profiles are shown since after a certain point, the membrane comes in contact with the rigid ends of the cylinder at top and bottom (see Figure 1). Dashed portions in Figure 7 depict the presence of uniformly distributed infinitesimally small wrinkles aligned with the meridional direction. As the inflation progresses inward, percentage of the wrinkled area reduces.

In the presence of an external magnetic field or when there is an electric current in the wire at $u = -1$, inward inflation may be seen even at positive values of net internal pressure P. However, the extent of deformation will be comparatively small since the membrane can only get so close to the membrane as explained later in section 5.3.1. In addition, multiple stable equilibrium states are possible for a given internal pressure and magnetic field as shown in Figure 8. We also note that the two solutions presented in Figure 8 are obtained numerically and unless rigorously proven mathematically we can't comment whether these are exhaustive. Same can be said for all the coupled field analyses in this study.

5.3.1 Magnetic limit point

Figure 9 shows some deformed profiles of a cylinder of aspect ratio $L_a = 6$ under the influence of magnetic field alone. Since the magnetic field is aligned with circumferential direction Θ, the membrane gets shrunk along the Θ direction thereby moving inward i.e., towards the wire at $u = -1$. We plot the curves by increasing the strength of the magnetic field (or value of $\mathcal{M}$)

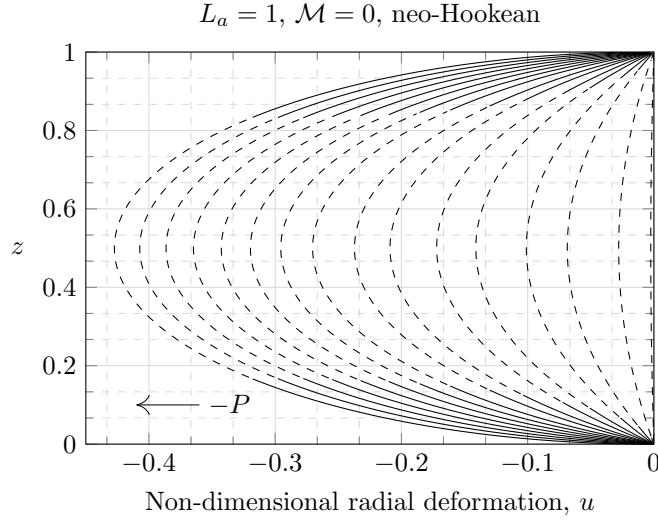28

$L_a = 1$, $\mathcal{M} = 0$, neo-Hookean

Figure 7: Deformed profiles of the cylindrical membrane under inward inflation. Solid and dashed parts represent unwrinkled and wrinkled regions, respectively. Arrow indicates the direction of increase in external pressure, $-P$. As the inflation progresses, ratio of the areas of the membrane with and without wrinkling decreases. Since all the models under consideration predict the same behaviour, only the results for neo-Hookean model are shown here.

Table 2: Radial deformations of a cylinder of $L_a = 6$ at mid-length at the magnetic limit point

$P(\times 10^{-4})$	$u\,(Z = L_a/2)$
0	-0.5473
1	-0.5445
2	-0.5391
3	-0.5363
4	-0.5336
6	-0.5289
8	-0.5225
10	-0.5200

until an increase in $\mathcal{M}$ can not yield an equilibrium state anymore.

Below this maximum possible value of $\mathcal{M}$ (the magnetic limit point) denoted henceforth by $\mathcal{M}_{lp}$, some values of $\mathcal{M}$ can give two corresponding stable equilibrium states as can be seen in Figure 9. Numerical values of $\mathcal{M}$ far below $\mathcal{M}_{lp}$ have only one corresponding equilibrium state located farther from the current carrying wire i.e., to the right of the critical state.

Increasing the value of $\mathcal{M}$ moves the inner-most deformed state outward and the outer-most state inward as depicted in Figure 9 by the two arrows. The deformed states from both the sides merge at 'magnetic limit point' associated with the maximum possible value of the dimensionless magnetic energy parameter $\mathcal{M}_{lp}$. A similar phenomenon was observed by Barham et al. (2008) in parametric deformation of a magnetoelastic circular membrane under the influence

29

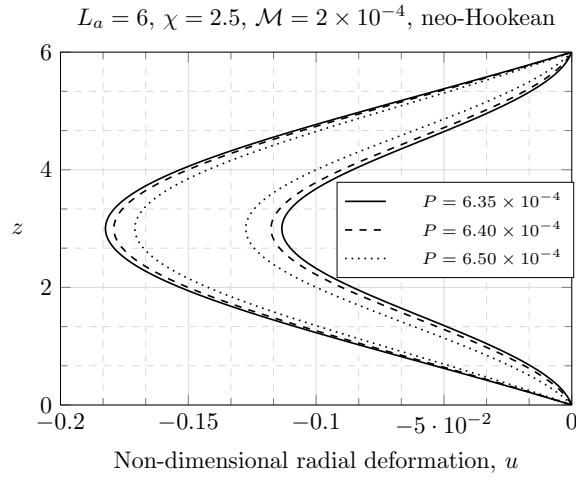$L_a = 6$, $\chi = 2.5$, $\mathcal{M} = 2 \times 10^{-4}$, neo-Hookean

Figure 8: Deformation profiles of the membrane for three different values of inflating pressure. Each curve represents a static equilibrium state. Another equilibrium state, corresponding to outward inflation, for each of these pressure values significantly coincides with the vertical axis at $u = 0$.

of a magnetic dipole. However, unlike their results, static equilibrium states obtained here are all stable. Also, in our previous study on a toroidal membrane (Reddy and Saxena, 2017), we reported a situation where, beyond a certain value of the magnetic energy parameter, both the stable and unstable equilibrium states cease to exist.

As can be predicted by intuition, presence of gas inside the membrane demands a stronger magnetic field for a given deformation and decreases the magnitude of radial deformation for a given current in the wire or $\mathcal{M}$. In addition, the equilibrium state corresponding to the magnetic limit point moves outward (away from the wire at $u = -1$) with the introduction of internal gas pressure as shown in Table 2 for $L_a = 6$.

A non-intuitive outcome of this study is the quadratic relation between the internal gas pressure and the corresponding value of the magnetic energy parameter $\mathcal{M}_{lp}$ corresponding to the magnetic limit point(see Figure 10). Reason for this result is not yet clear. Though only two aspect ratios of the cylinder are shown in Figure 10, similar results are obtained for other aspect ratios. Cylinders shorter than $L_a = 1$ are not commented upon since they call for unreasonably high values of current in the wire (see eqn. 44, Figure 5). We also note that the order of magnitudes of $\mathcal{M}_{lp}$ and P are the same in Figure 10.

Figure 10 also specifies the minimum amount of internal pressure required to deform the membrane for a given $\mathcal{M}$ and the maximum amount of $\mathcal{M}$ allowed for an internal pressure
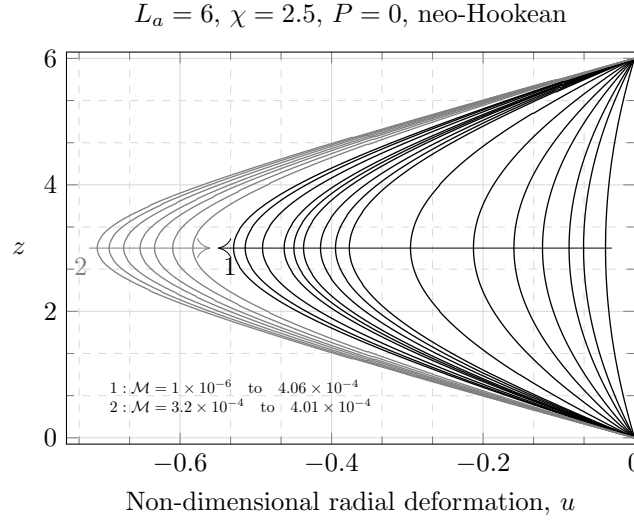
$L_a = 6$, $\chi = 2.5$, $P = 0$, neo-Hookean

Figure 9: Deformation profiles of the cylindrical membrane under the influence of magnetic field alone ($P = 0$). The arrows indicate the direction of increase in $\mathcal{M}$. Solutions from both the directions merge at the magnetic limit point and the corresponding value of the magnetic energy density parameter: $\mathcal{M} \approx 4.07 \times 10^{-4}$. This position moves away from the wire (located at $u = -1$) with increase in internal pressure. Not every value of $\mathcal{M}$ has two corresponding stable solutions.

P. For example, at $\mathcal{M} = 0.3$ for $L_a = 1$, internal pressure P must be greater than 0.7, approximately to yield an equilibrium solution (Figure 10a). Connecting this inference with the pressure-stretch plot for $\mathcal{M} = 0.3$ in Figure 5c or Figure 5e, we understand that there are not many solutions to the left of the pressure-stretch plots in Figure 5 due to the presence of magnetic limit point as illustrated in Figure 9.

6   Conclusions

The effect of an external magnetic field on the inflation of a cylindrical membrane is studied. A variational formulation based on magnetization and a finite difference method are used to obtain equilibrium solutions. Stability of the equilibrium states is determined from the second variation while the onset of wrinkling instability is determined using relaxed energy density approach. The strain energy density is expressed using four models: neo-Hookean, Mooney-Rivlin, Ogden and series expansion form of Arruda-Boyce and the results are compared. It is observed that all these constitutive models except the Mooney-Rivlin model predict bulging in long cylinders. While these models lead to significantly different pressure-stretch plots for outward inflation, there is not much difference in case of inward inflation i.e., when the internal pressure is less than the external pressure. Inward inflation also causes portions of the membrane to wrinkle and as inflation progresses inward, the percentage of wrinkled area reduces.
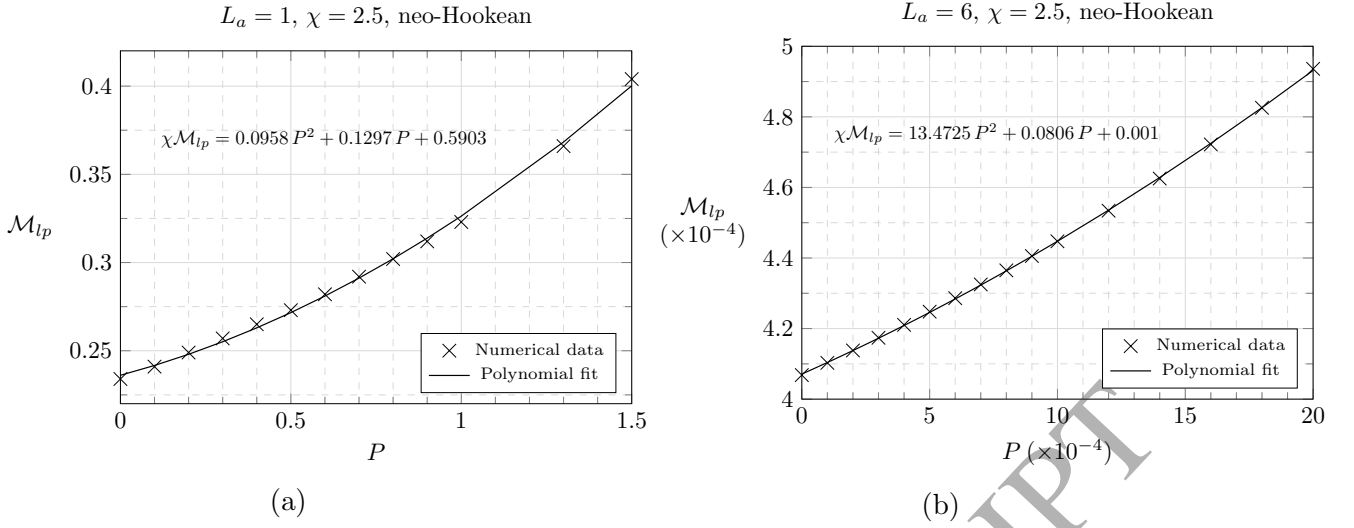
31

Figure 10: Variation of the magnetic energy density parameter at magnetic limit point, $\mathcal{M}_{lp}$ with the inflating internal pressure P for the aspect ratio (a) $L_a = 1$ and (b) $L_a = 6$. The numerical values of $\mathcal{M}_{lp}$ and P (marked as ×) are closely related by a polynomial of order 2 (solid line).

In the presence of an external magnetic field, pressure-stretch curve starts at a non-zero value of inflating pressure and for certain aspect ratios of the cylinder, an initial dip in the inflating pressure is seen. For a sufficiently strong magnetic field, this initial dip disappears and the net internal pressure falls monotonously. Current in the wire at the axis of symmetry can be increased only so much before a further increase yields no equilibrium solutions. This critical state is termed the magnetic limit point. Below this maximum value, a value of current (but not those much smaller than the maximum value) has two corresponding deformed solutions one on either side of the magnetic limit point. A highlight of this study is the polynomial relation between the defined magnetic energy parameter and the inflating pressure at magnetic limit point.

Possible extensions of this study can be to improve the employed numerical scheme which is sensitive to the initial guess provided, and an improvement of the second variation analysis to accommodate more stable solutions. Also, inflation of a strongly magnetized membrane may be studied i.e., without neglecting the material's self generated magnetic field.

Funding statement

A Appendix

The partial derivatives of the integrand $\mathcal{F}$ mentioned in Sec. 3.3.1 are as follows, multiplied by a factor $\mu T R_0^2$ which is a constant for given material and geometry.

$$\mathcal{F}_{u'} = \frac{1}{\mu} \frac{\partial \widehat{W}}{\partial \lambda_1} \frac{\partial \lambda_1}{\partial u'}, \qquad \mathcal{F}_{w'} = \frac{1}{\mu} \frac{\partial \widehat{W}}{\partial \lambda_1} \frac{\partial \lambda_1}{\partial w'} - \frac{1}{2} P(1+u)^2, \tag{67}$$

$$\mathcal{F}_{u'u'} = \frac{1}{\mu} \left[\frac{\partial}{\partial \lambda_1} \left(\frac{\partial \widehat{W}}{\partial \lambda_1} \right) \left[\frac{\partial \lambda_1}{\partial u'} \right]^2 + \frac{\partial \widehat{W}}{\partial \lambda_1} \frac{\partial}{\partial u'} \left(\frac{\partial \lambda_1}{\partial u'} \right) \right], \tag{68}$$

$$\mathcal{F}_{u'w'} = \mathcal{F}_{w'u'} = \frac{1}{\mu} \left[\frac{\partial}{\partial \lambda_1} \left(\frac{\partial \widehat{W}}{\partial \lambda_1} \right) \frac{\partial \lambda_1}{\partial w'} \frac{\partial \lambda_1}{\partial u'} + \frac{\partial \widehat{W}}{\partial \lambda_1} \frac{\partial}{\partial w'} \left(\frac{\partial \lambda_1}{\partial u'} \right) \right], \tag{69}$$

$$\mathcal{F}_{w'w'} = \frac{1}{\mu} \left[\frac{\partial}{\partial \lambda_1} \left(\frac{\partial \widehat{W}}{\partial \lambda_1} \right) \left(\frac{\partial \lambda_1}{\partial w'} \right)^2 + \frac{\partial \widehat{W}}{\partial \lambda_1} \frac{\partial}{\partial w'} \left(\frac{\partial \lambda_1}{\partial w'} \right) \right], \tag{70}$$

$$\mathcal{F}_u = \frac{1}{\mu} \frac{\partial \widehat{W}}{\partial \lambda_2} + \frac{\chi \mathcal{M}}{[1+u]^3} - P[1+u][1+w'], \tag{71}$$

$$\mathcal{F}_{uu} = \frac{1}{\mu} \frac{\partial}{\partial \lambda_2} \left(\frac{\partial \widehat{W}}{\partial \lambda_2} \right) - \frac{3\chi \mathcal{M}}{[1+u]^4} - P[1+w'], \tag{72}$$

$$\mathcal{F}_w = \mathcal{F}_{wu} = \mathcal{F}_{uw} = \mathcal{F}_{ww} = 0, \tag{73}$$

$$\mathcal{F}_{uu'} = \frac{1}{\mu} \frac{\partial}{\partial \lambda_1} \left(\frac{\partial \widehat{W}}{\partial \lambda_2} \right) \frac{\partial \lambda_1}{\partial u'}, \qquad \mathcal{F}_{uw'} = \frac{1}{\mu} \frac{\partial}{\partial \lambda_1} \left(\frac{\partial \widehat{W}}{\partial \lambda_2} \right) \frac{\partial \lambda_1}{\partial w'} - P[1+u], \tag{74}$$

$$\mathcal{F}_{wu'} = \mathcal{F}_{ww'} = 0. \tag{75}$$

$$\frac{\mathrm{d}}{\mathrm{d}Z} \mathcal{F}_{uu'} = \frac{\mathrm{d}\mathcal{A}}{\mathrm{d}Z} \left[\frac{u'}{\lambda_1} \right] + \mathcal{A} \frac{\mathrm{d}}{\mathrm{d}Z} \left(\frac{u'}{\lambda_1} \right), \qquad \frac{\mathrm{d}}{\mathrm{d}Z} \mathcal{F}_{uw'} = \frac{\mathrm{d}\mathcal{A}}{\mathrm{d}Z} \left[\frac{1+w'}{\lambda_1} \right] + \mathcal{A} \frac{\mathrm{d}}{\mathrm{d}Z} \left(\frac{1+w'}{\lambda_1} \right), \tag{76}$$

$$\frac{\mathrm{d}}{\mathrm{d}Z} \mathcal{F}_{u'u'} = \frac{\mathrm{d}\mathcal{I}}{\mathrm{d}Z} \left[\frac{u'}{\lambda_1} \right]^2 + \mathcal{I} \frac{\mathrm{d}}{\mathrm{d}Z} \left(\left[\frac{u'}{\lambda_1} \right]^2 \right) + \frac{\mathrm{d}\mathcal{U}}{\mathrm{d}Z} \left[\frac{[1+w']^2}{\lambda_1^3} \right] + \mathcal{U} \frac{\mathrm{d}}{\mathrm{d}Z} \left(\frac{[1+w']^2}{\lambda_1^3} \right), \tag{77}$$

$$\frac{\mathrm{d}}{\mathrm{d}Z} \mathcal{F}_{w'w'} = \frac{\mathrm{d}\mathcal{I}}{\mathrm{d}Z} \left[\frac{1+w'}{\lambda_1} \right]^2 + \mathcal{I} \frac{\mathrm{d}}{\mathrm{d}Z} \left(\left[\frac{1+w'}{\lambda_1} \right]^2 \right) + \frac{\mathrm{d}\mathcal{U}}{\mathrm{d}Z} \left[\frac{u'^2}{\lambda_1^3} \right] + \mathcal{U} \frac{\mathrm{d}}{\mathrm{d}Z} \left(\frac{u'^2}{\lambda_1^3} \right), \tag{78}$$

$$\frac{\mathrm{d}}{\mathrm{d}Z} \mathcal{F}_{u'w'} = \frac{\mathrm{d}\mathcal{I}}{\mathrm{d}Z} \left[\frac{u'[1+w']}{\lambda_1^2} \right] + \mathcal{I} \frac{\mathrm{d}}{\mathrm{d}Z} \left(\frac{u'[1+w']}{\lambda_1^2} \right) - \frac{\mathrm{d}\mathcal{U}}{\mathrm{d}Z} \left[\frac{u'[1+w']}{\lambda_1^3} \right] - \mathcal{U} \frac{\mathrm{d}}{\mathrm{d}Z} \left(\frac{u'[1+w']}{\lambda_1^3} \right). \tag{79}$$

$$\mathcal{A} = \frac{1}{\mu} \frac{\partial^2 \widehat{W}}{\partial \lambda_1 \lambda_2}, \qquad \mathcal{I} = \frac{1}{\mu} \frac{\partial^2 \widehat{W}}{\partial \lambda_1^2}, \qquad \mathcal{U} = \frac{1}{\mu} \frac{\partial \widehat{W}}{\partial \lambda_1}. \tag{80}$$

Expressions for the partial derivatives of the Ogden's strain energy function (see Sec. 3.2.1) are as follows

$$\frac{\partial \widehat{W}}{\partial \lambda_i} = \sum_{k=1}^{K} \mu_k \left[\lambda_i^{\alpha_k-1} - \left[\frac{1}{\lambda_1 \lambda_2} \right]^{\alpha_k} \frac{1}{\lambda_i} \right] \tag{81a}$$

$$\frac{\partial^2 \widehat{W}}{\partial \lambda_i^2} = \sum_{k=1}^{K} \mu_k \left[[\alpha_k - 1] \lambda_i^{\alpha_k-2} + \left[\frac{1}{\lambda_1 \lambda_2} \right]^{\alpha_k} \left[\frac{\alpha_k + 1}{\lambda_i^2} \right] \right] \tag{81b}$$

$$\frac{\partial^2 \widehat{W}}{\partial \lambda_1 \partial \lambda_2} = \sum_{k=1}^{K} \mu_k \left[\frac{\alpha_k}{[\lambda_1 \lambda_2]^{\alpha_k+1}} \right], \tag{81c}$$

$$\frac{\partial}{\partial \lambda_i} \left(\frac{\partial^2 \widehat{W}}{\partial \lambda_1 \partial \lambda_2} \right) = - \sum_{k=1}^{K} \mu_k \frac{\alpha_k [\alpha_k + 1]}{[\lambda_1 \lambda_2]^{\alpha_k+1}} \frac{1}{\lambda_i}, \tag{81d}$$

$$\frac{\partial}{\partial \lambda_1} \left(\frac{\partial^2 \widehat{W}}{\partial \lambda_1^2} \right) = \sum_{k=1}^{K} \mu_k \left[[\alpha_k - 1] [\alpha_k - 2] \lambda_1^{\alpha_k-3} - \frac{[\alpha_k + 1] [\alpha_k + 2]}{\lambda_2^{\alpha_k} \lambda_1^{\alpha_k+3}} \right], \tag{81e}$$

$$\frac{\partial}{\partial \lambda_2} \left(\frac{\partial^2 \widehat{W}}{\partial \lambda_1^2} \right) = \frac{\partial}{\partial \lambda_1} \left(\frac{\partial^2 \widehat{W}}{\partial \lambda_1 \partial \lambda_2} \right), \tag{81f}$$

$$\frac{\mathrm{d}}{\mathrm{d}Z} \left(\frac{\partial \widehat{W}}{\partial \lambda_1} \right) = \sum_{k=1}^{K} \mu_k \left[[\alpha_k - 1] \lambda_1^{\alpha_k-2} \lambda_1' + [\alpha_k + 1] \frac{\lambda_1'}{\lambda_1^2} \left[\frac{1}{\lambda_1 \lambda_2} \right]^{\alpha_k} + \alpha_k \lambda_2' \left[\frac{1}{\lambda_1 \lambda_2} \right]^{\alpha_k+1} \right]. \tag{82}$$

In the case of wrinkling in the circumferential direction,

$$\widehat{W}_r = \sum_{k=1}^{K} \frac{\mu_k}{\alpha_k} \left[\lambda_1^{\alpha_k} + 2\lambda_1^{-\frac{\alpha_k}{2}} - 3 \right], \tag{83}$$

$$\frac{\partial \widehat{W}_r}{\partial \lambda_1} = \sum_{k=1}^{K} \mu_k \left[\lambda_1^{\alpha_k-1} - \lambda_1^{-\frac{\alpha_k}{2}-1} \right], \tag{84}$$

$$\frac{\partial^2 \widehat{W}_r}{\partial \lambda_1^2} = \sum_{k=1}^{K} \mu_k \left[[\alpha_k - 1] \lambda_1^{\alpha_k-2} + \left[\frac{\alpha_k}{2} + 1 \right] \lambda_1^{-\frac{\alpha_k}{2}-2} \right], \tag{85}$$

$$\frac{\partial^3 \widehat{W}_r}{\partial \lambda_1^3} = \sum_{k=1}^{K} \mu_k \left[[\alpha_k - 1] [\alpha_k - 2] \lambda_1^{\alpha_k-3} - \left[\frac{\alpha_k}{2} + 1 \right] \left[\frac{\alpha_k}{2} + 2 \right] \lambda_1^{-\frac{\alpha_k}{2}-3} \right], \tag{86}$$

with the derivative of any quantity with respective to the circumferential stretch, λ_2 being identically equal to zero. Similarly, those corresponding to the Arruda-Boyce strain energy

34

density function mentioned in Sec. 3.2.4 are

$$\frac{\partial \widehat{W}}{\partial \lambda_i} = I_{1,\lambda_i} \mathcal{S}_1, \tag{87}$$

$$\frac{\partial^2 \widehat{W}}{\partial \lambda_i^2} = 2\left[1 + \frac{3}{[\lambda_1 \lambda_2]^2} \frac{1}{\lambda_i^2}\right] \mathcal{S}_1 + [I_{1,\lambda_i}]^2 \mathcal{S}_2, \tag{88}$$

$$\frac{\partial^2 \widehat{W}}{\partial \lambda_1 \partial \lambda_2} = \frac{4}{[\lambda_1 \lambda_2]^3} \mathcal{S}_1 + I_{1,\lambda_1} I_{1,\lambda_2} \mathcal{S}_2, \tag{89}$$

$$\frac{\partial}{\partial \lambda_1}\left(\frac{\partial^2 \widehat{W}}{\partial \lambda_1^2}\right) = \frac{-24}{\lambda_2^2 \lambda_1^5} \mathcal{S}_1 + 6\, I_{1,\lambda_1}\left[1 + \frac{3}{\lambda_2^2 \lambda_1^4}\right] \mathcal{S}_2 + [I_{1,\lambda_1}]^3 \mathcal{S}_3, \tag{90}$$

$$\frac{\partial}{\partial \lambda_1}\left(\frac{\partial^2 \widehat{W}}{\partial \lambda_1 \partial \lambda_2}\right) = \frac{-12}{\lambda_2^3 \lambda_1^4} \mathcal{S}_1 + \frac{8}{[\lambda_1 \lambda_2]^3} \mathcal{S}_2 [I_{1,\lambda_1}] + 2\left[1 + \frac{3}{\lambda_2^2 \lambda_1^4}\right] I_{1,\lambda_2} \mathcal{S}_2 + I_{1,\lambda_1} I_{1,\lambda_2} \mathcal{S}_3 [I_{1,\lambda_1}], \tag{91}$$

$$\frac{\partial}{\partial \lambda_2}\left(\frac{\partial^2 \widehat{W}}{\partial \lambda_1 \partial \lambda_2}\right) = \frac{-12}{\lambda_1^3 \lambda_2^4} \mathcal{S}_1 + \frac{8}{[\lambda_1 \lambda_2]^3} \mathcal{S}_2 [I_{1,\lambda_2}] + 2\left[1 + \frac{3}{\lambda_1^2 \lambda_2^4}\right] I_{1,\lambda_1} \mathcal{S}_2 + I_{1,\lambda_1} I_{1,\lambda_2} \mathcal{S}_3 [I_{1,\lambda_2}], \tag{92}$$

$$\frac{\mathrm{d}}{\mathrm{d}Z}\left(\frac{\partial \widehat{W}}{\partial \lambda_1}\right) = 2\left[\lambda_1' + \frac{2\frac{\lambda_2'}{\lambda_2} + 3\frac{\lambda_1'}{\lambda_1}}{\lambda_2^2 \lambda_1^3}\right] \mathcal{S}_1 + I_{1,\lambda_1} \mathcal{S}_2 (I_{1,Z}), \tag{93}$$

$$\mathcal{S}_1 = \mu \sum_{k=1}^{K} \frac{k\, c_k\, I_1^{k-1}}{N^{k-1}}, \quad \mathcal{S}_2 = \mu \sum_{k=1}^{K} \frac{k\,[k-1]\, c_k\, I_1^{k-2}}{N^{k-1}}, \quad \mathcal{S}_3 = \mu \sum_{k=1}^{K} \frac{k\,[k-1]\,[k-2]\, c_k\, I_1^{k-3}}{N^{k-1}} \tag{94}$$

where

$$I_{1,Z} = 2\left[\lambda_1 \lambda_1' + \lambda_2 \lambda_2' - \frac{\lambda_1'}{\lambda_1}\left[\frac{1}{\lambda_1 \lambda_2}\right]^2 - \frac{\lambda_2'}{\lambda_2}\left[\frac{1}{\lambda_1 \lambda_2}\right]^2\right], \tag{95}$$

$$I_{1,\lambda_1} = 2\left[\lambda_1 - \frac{1}{\lambda_2^2 \lambda_1^3}\right], \qquad I_{1,\lambda_2} = 2\left[\lambda_2 - \frac{1}{\lambda_1^2 \lambda_2^3}\right]. \tag{96}$$

In the case of wrinkling in the circumferential direction,

$$I_1 = \lambda_1^2 + \frac{2}{\lambda_1}, \qquad \frac{\partial I_1}{\partial \lambda_1} = 2\left[\lambda_1 - \frac{1}{\lambda_1^2}\right], \qquad \frac{\partial^2 I_1}{\partial \lambda_1^2} = 2\left[1 + \frac{2}{\lambda_1^3}\right], \qquad \frac{\partial^3 I_1}{\partial \lambda_1^3} = -\frac{12}{\lambda_1^4}, \tag{97}$$

$$\frac{\partial \widehat{W}_r}{\partial \lambda_1} = \mathcal{S}_1 \frac{\partial I_1}{\partial \lambda_1}, \quad \frac{\partial^2 \widehat{W}_r}{\partial \lambda_1^2} = \mathcal{S}_2 \left[\frac{\partial I_1}{\partial \lambda_1}\right]^2 + \mathcal{S}_1 \frac{\partial^2 I_1}{\partial \lambda_1^2}, \quad \frac{\partial^3 \widehat{W}_r}{\partial \lambda_1^3} = \mathcal{S}_3 \left[\frac{\partial I_1}{\partial \lambda_1}\right]^3 + 3\mathcal{S}_2 \frac{\partial^2 I_1}{\partial \lambda_1^2}\frac{\partial I_1}{\partial \lambda_1} + \mathcal{S}_1 \frac{\partial^3 I_1}{\partial \lambda_1^3}. \tag{98}$$

References

Alexander H. "Tensile instability of initially spherical balloons". *International Journal of Engineering Science*, 9(1):151–160 (1971)

Arruda E.M. and Boyce M.C. "A three-dimensional constitutive model for the large stretch behavior of rubber elastic materials". *Journal of the Mechanics and Physics of Solids*, 41(2):389–412 (1993)

Barham M., Steigmann D.J., McElfresh M., and Rudd R.E. "Finite deformation of a pressurized magnetoelastic membrane in a stationary dipole field". *Acta Mechanica*, 191(1-2):1–19 (2007)

Barham M., Steigmann D.J., McElfresh M., and Rudd R.E. "Limit-point instability of a magnetoelastic membrane in a stationary magnetic field". *Smart Materials and Structures*, 17(5):055003 (2008)

Benedict R., Wineman A., and Yang W.H. "The determination of limiting pressure in simultaneous elongation and inflation of nonlinear elastic tubes". *International Journal of Solids and Structures*, 15(3):241–249 (1979)

Bense H., Trejo M., Reyssat E., Bico J., and Roman B. "Buckling of elastomer sheets under non-uniform electro-actuation". *Soft Matter*, 13(15):2876–2885 (2017)

Bischoff J.E., Arruda E.M., and Grosh K. "Finite element modeling of human skin using an isotropic, nonlinear elastic constitutive model". *Journal of Biomechanics*, 33(6):645–652 (2000)

Böse H., Rabindranath R., and Ehrlich J. "Soft magnetorheological elastomers as new actuators for valves". *Journal of Intelligent Material Systems and Structures*, page 1045389X11433498 (2012)

Böse H. and Röder R. "Magnetorheological elastomers with high variability of their mechanical properties". *In* "Journal of physics: Conference Series", volume 149, page 012090. IOP Publishing (2009)

Boyce M.C. and Arruda E.M. "Constitutive models of rubber elasticity: a review". *Rubber chemistry and technology*, 73(3):504–523 (2000)

Brigadnov I.A. and Dorfmann A. "Mathematical modeling of magneto-sensitive elastomers". *International Journal of Solids and Structures*, 40(18):4659–4674 (2003)

Brown W.F. *Magnetoelastic interactions.* Springer, New York (1966)

Bustamante R. "Transversely isotropic nonlinear magneto-active elastomers". *Acta Mechanica*, 210(3-4):183–214 (2010)

Castañeda P.P. and Galipeau E. "Homogenization-based constitutive models for magnetorheological elastomers at finite strain". *Journal of the Mechanics and Physics of Solids*, 59(2):194–215 (2011)

Chatzigeorgiou G., Javili A., and Steinmann P. "Unified magnetomechanical homogenization framework with application to magnetorheological elastomers". *Mathematics and Mechanics of Solids*, 19(2):193–211 (2014)

Danas K., Kankanala S., and Triantafyllidis N. "Experiments and modeling of iron-particle-filled magnetorheological elastomers". *Journal of the Mechanics and Physics of Solids*, 60(1):120–138 (2012)

Danas K. and Triantafyllidis N. "Instability of a magnetoelastic layer resting on a non-magnetic substrate". *Journal of the Mechanics and Physics of Solids*, 69:67–83 (2014)

Dorfmann A. and Ogden R.W. "Magnetoelastic modelling of elastomers". *European Journal of Mechanics- A/Solids*, 22(4):497–507 (2003)

Dorfmann A. and Ogden R.W. "Some problems in nonlinear magnetoelasticity". *Zeitschrift für angewandte Mathematik und Physik*, 56(4):718–745 (2005)

Dorfmann L. and Ogden R.W. *Nonlinear Theory of Electroelastic and Magnetoelastic Interactions.* Springer, New York (2014)

Epstein M. "On the wrinkling of anisotropic elastic membranes". *Journal of Elasticity*, 55(2):99–109 (1999)

Ethiraj G. and Miehe C. "Multiplicative magneto-elasticity of magnetosensitive polymers incorporating micromechanically-based network kernels". *International Journal of Engineering Science*, 102:93 – 119 (2016)

Farshad M. and Benine A. "Magnetoactive elastomer composites". *Polymer Testing*, 23(3):347–353 (2004)

Fox J.W. and Goulbourne N.C. "On the dynamic electromechanical loading of dielectric elastomer membranes". *Journal of the Mechanics and Physics of Solids*, 56(8):2669–2686 (2008)

Fox J.W. and Goulbourne N.C. "Electric field-induced surface transformations and experimental dynamic characteristics of dielectric elastomer membranes". *Journal of the Mechanics and Physics of Solids*, 57(8):1417–1435 (2009)

Galipeau E. and Castañeda P.P. "Giant field-induced strains in magnetoactive elastomer composites". *Proceedings of the Royal Society A*, 469:20130385 (2013)

Gelfand I.M. and Fomin S.V. *Calculus of Variations,(Translated and edited by Silverman, RA).* Dover Edition (2000)

Gent A.N. "Elastic instabilities of inflated rubber shells". *Rubber chemistry and technology*, 72(2):263–268 (1999)

Gent A.N. "Elastic instabilities in rubber". *International Journal of Non-Linear Mechanics*, 40(2):165–175 (2005)

Ginder J.M., Clark S.M., Schlotter W.F., and Nichols M.E. "Magnetostrictive phenomena in magnetorheological elastomers". *International Journal of Modern Physics B*, 16(17n18):2412–2418 (2002)

Ginder J.M., Schlotter W.F., and Nichols M.E. "Magnetorheological elastomers in tunable vibration absorbers". *In* "SPIE's 8th Annual International Symposium on Smart Structures and Materials", pages 103–110. International Society for Optics and Photonics (2001)

Gong X.L., Zhang X.Z., and Zhang P.Q. "Fabrication and characterization of isotropic magnetorheological elastomers". *Polymer testing*, 24(5):669–676 (2005)

Goshkoderia A. and Rudykh S. "Stability of magnetoactive composites with periodic microstructures undergoing finite strains in the presence of a magnetic field". *Composites Part B: Engineering*, 128(Supplement C):19 – 29 (2017)

Grossman G. "Analysis of rim supports for off-axis inflatable reflectors. i: Loads". *Journal of Aerospace Engineering*, 4(1):47–66 (1991a)

Grossman G. "Analysis of rim supports for off-axis inflatable reflectors. ii: Deformations". *Journal of Aerospace Engineering*, 4(1):67–77 (1991b)

Grossman G. "Tension element to reduce loads in rim support of inflatable reflector". *Journal of Aerospace Engineering*, 7(2):129–142 (1994)

Haldar K., Kiefer B., and Menzel A. "Finite element simulation of rate-dependent magnetoactive polymer response". *Smart Materials and Structures*, 25(10):104003 (2016)

Haughton D.M. and McKay B.A. "Wrinkling of annular discs subjected to radial displacements". *International journal of engineering science*, 33(3):335–350 (1995)

38

Haughton D.M. and Ogden R.W. "Bifurcation of inflated circular cylinders of elastic material under axial loading–i. membrane theory for thin-walled tubes". *Journal of the Mechanics and Physics of Solids*, 27(3):179–212 (1979)

Jedynak R. "Approximation of the inverse langevin function revisited". *Rheologica Acta*, 54(1):29–39 (2015)

Jolly M.R., Carlson J.D., and Munoz B.C. "A model of the behaviour of magnetorheological materials". *Smart Materials and Structures*, 5(5):607 (1996)

Kankanala S.V. and Triantafyllidis N. "On finitely strained magnetorheological elastomers". *Journal of the Mechanics and Physics of Solids*, 52(12):2869–2908 (2004)

Kankanala S.V. and Triantafyllidis N. "Magnetoelastic buckling of a rectangular block in plane strain". *Journal of the Mechanics and Physics of Solids*, 56:1147–1169 (2008)

Kanner L.M. and Horgan C.O. "Elastic instabilities for strain-stiffening rubber-like spherical and cylindrical thin shells under inflation". *International Journal of Non-Linear Mechanics*, 42(2):204–215 (2007)

Keh L.O.S.C.T., Zang J., and Zhao X. "Magneto-rheological foams capable of tunable energy absorption". *In* "2013 Proceedings of IEEE Southeastcon", pages 1–3 (2013)

Keplinger C., Li T., Baumgartner R., Suo Z., and Bauer S. "Harnessing snap-through instability in soft dielectrics to achieve giant voltage-triggered deformation". *Soft Matter*, 8(2):285–288 (2012)

Khayat R.E., Derdorri A., Garcia-R A. et al. "Inflation of an elastic cylindrical membrane: non-linear deformation and instability". *International Journal of Solids and Structures*, 29(1):69–87 (1992)

Khayat R.E. and Derdouri A. "Inflation of hyperelastic cylindrical membranes as applied to blow moulding. part i. axisymmetric case". *International Journal for Numerical Methods in Engineering*, 37(22):3773–3791 (1994a)

Khayat R.E. and Derdouri A. "Inflation of hyperelastic cylindrical membranes as applied to blow moulding. part ii. non-axisymmetric case". *International Journal for Numerical Methods in Engineering*, 37(22):3793–3808 (1994b)

Khayat R.E., Derdouri A., and García-Rejón A. "Multiple contact and axisymmetric inflation of hyperelastic cylindrical membranes". *Proceedings of the Institution of Mechanical Engineers, Part C: Journal of Mechanical Engineering Science*, 207(3):175–183 (1993)

Krautz M., Werner D., Schrödner M., Funk A., Jantz A., Popp J., Eckert J., and Waske A. "Hysteretic behavior of soft magnetic elastomer composites". *Journal of Magnetism and Magnetic Materials*, 426:60–63 (2017)

Kydoniefs A.D. and Spencer A.J.M. "Finite axisymmetric deformations of an initially cylindrical elastic membrane". *The Quarterly Journal of Mechanics and Applied Mathematics*, 22(1):87–95 (1969)

Kyriakides S. and Yu-Chung C. "The initiation and propagation of a localized instability in an inflated elastic tube". *International Journal of Solids and Structures*, 27(9):1085–1111 (1991)

Leone J.E. "Infusion balloon catheter" (1994). US Patent 5,318,531

Li T., Keplinger C., Baumgartner R., Bauer S., Yang W., and Suo Z. "Giant voltage-induced deformation in dielectric elastomers near the verge of snap-through instability". *Journal of the Mechanics and Physics of Solids*, 61(2):611–628 (2013)

Li X. and Steigmann D.J. "Finite deformation of a pressurized toroidal membrane". *International Journal of Non-Linear Mechanics*, 30(4):583–595 (1995a)

Li X. and Steigmann D.J. "Point loads on a hemispherical elastic membrane". *International Journal of Non-Linear Mechanics*, 30(4):569–581 (1995b)

Mansfield E.H. "Gravity-induced wrinkle lines in vertical membranes". *In* "Proceedings of the Royal Society of London A: Mathematical, Physical and Engineering Sciences", volume 375, pages 307–325. The Royal Society (1981)

Marckmann G. and Verron E. "Comparison of hyperelastic models for rubber-like materials". *Rubber Chemistry and Technology*, 79(5):835–858 (2006)

Maugin G.A. and Eringen A.C. "Deformable magnetically saturated media. i. field equations". *Journal of Mathematical Physics*, 13(2):143–155 (1972)

Mayer M., Rabindranath R., Börner J., Hörner E., Bentz A., Salgado J., Han H., Böse H., Probst J., Shamonin M., Monkman G.J., and Schlunck G. "Ultra-Soft PDMS-Based Magnetoactive Elastomers as Dynamic Cell Culture Substrata." *PloS one*, 8(10):e76196 (2013)

Ogden R.W. "Large deformation isotropic elasticity – on the correlation of theory and experiment for incompressible rubberlike solids". *In* "Proceedings of the Royal Society of London A: Mathematical, Physical and Engineering Sciences", volume 326, pages 565–584 (1972)

Ogden R.W. and Steigmann D.J. (Eds.). *Mechanics and Electrodynamics of Magneto- and Electro-Elastic Materials*, volume 527. SpringerWeinNewYork (2011)

Otténio M., Destrade M., and Ogden R.W. "Incremental magnetoelastic deformations, with application to surface instability". *Journal of Elasticity*, 90(1):19–42 (2008)

Pamplona D., Gonçalves P., Davidovich M., and Weber H.I. "Finite axisymmetric deformations of an initially stressed fluid-filled cylindrical membrane". *International Journal of Solids and Structures*, 38(10):2033–2047 (2001)

Pamplona D.C., Goncalves P.B., and Lopes S.R.X. "Finite deformations of cylindrical membrane under internal pressure". *International Journal of Mechanical Sciences*, 48(6):683–696 (2006)

Pao Y.H. "Electromagnetic forces in deformable continua". *In* "Mechanics today. Volume 4.(A78-35706 14-70) New York, Pergamon Press, Inc., 1978, p. 209-305. NSF-supported research.", volume 4, pages 209–305 (1978)

Pao Y.H. and Yeh C.S. "A linear theory for soft ferromagnetic elastic bodies". *International Journal of Engineering Science*, 11(4):415–436 (1973)

Patil A., Nordmark A., and Eriksson A. "Free and constrained inflation of a pre-stretched cylindrical membrane". *Proceedings of the Royal Society of London A: Mathematical, Physical and Engineering Sciences*, 470(2169) (2014)

Patil A., Nordmark A., and Eriksson A. "Instability investigation on fluid-loaded pre-stretched cylindrical membranes". *Proceedings of the Royal Society of London A: Mathematical, Physical and Engineering Sciences*, 471(2177) (2015a)

Patil A., Nordmark A., and Eriksson A. "Wrinkling of cylindrical membranes with non-uniform thickness". *European Journal of Mechanics-A/Solids*, 54:1–10 (2015b)

Pipkin A.C. "The relaxed energy density for isotropic elastic membranes". *IMA Journal of Applied Mathematics*, 36(1):85–99 (1986)

Rachik M., Schmidtt F., Reuge N., Le Maoult Y., and Abbeé F. "Elastomer biaxial characterization using bubble inflation technique. ii: Numerical investigation of some constitutive models". *Polymer Engineering & Science*, 41(3):532–541 (2001)

Raikher Y.L., Stolbov O.V., and Stepanov G.V. "Deformation of a circular ferroelastic membrane in a uniform magnetic field". *Technical Physics*, 53(9):1169–1176 (2008)

Reddy N.H. and Saxena P. "Limit points in the free inflation of a magnetoelastic toroidal membrane". *International Journal of Non-Linear Mechanics*, 95(C):248–263 (2017)

Rudykh S. and Bertoldi K. "Stability of anisotropic magnetorheological elastomers in finite deformations: A micromechanical approach". *Journal of the Mechanics and Physics of Solids*, 61(4):949 – 967 (2013)

Rudykh S., Bhattacharya K., and deBotton G. "Snap-through actuation of thick-wall electroactive balloons". *International Journal of Non-Linear Mechanics*, 47(2):206 – 209 (2012). Nonlinear Continuum Theories

Saxena P. "Finite deformations and incremental axisymmetric motions of a magnetoelastic tube". *Mathematics and Mechanics of Solids* (2017)

Saxena P., Hossain M., and Steinmann P. "A theory of finite deformation magneto-viscoelasticity". *International Journal of Solids and Structures*, 50(24):3886–3897 (2013)

Saxena P., Hossain M., and Steinmann P. "Nonlinear magneto-viscoelasticity of transversally isotropic magneto-active polymers". *Proceedings of the Royal Society A*, 470(2166):20140082 (2014)

Seibert D.J. and Schoche N. "Direct comparison of some recent rubber elasticity models". *Rubber chemistry and technology*, 73(2):366–384 (2000)

Skala D.P. "Modified equations of rubber elasticity applied to the inflation mechanics of a thick-walled rubber cylinder". *Rubber Chemistry and Technology*, 43(4):745–757 (1970)

Steigmann D. "Tension-field theory". *In* "Proceedings of the Royal Society A, 429", pages 141–173 (1990)

Steigmann D.J. "Equilibrium theory for magnetic elastomers and magnetoelastic membranes". *International Journal of Non-Linear Mechanics*, 39(7):1193–1216 (2004)

Steigmann D.J. and Pipkin A.C. "Finite deformations of wrinkled membranes". *The Quarterly Journal of Mechanics and Applied Mathematics*, 42(3):427–440 (1989)

Stein M. and Hedgepeth J.M. "Analysis of partly wrinkled membranes". techreport, Langley Research Center, Langley Field, Va. (1961)

Steinmann P., Hossain M., and Possart G. "Hyperelastic models for rubber-like materials: consistent tangent operators and suitability for Treloars data". *Archive of Applied Mechanics*, 82(9):1183–1217 (2012)

Tews A.M., Pope K.L., and Snyder A.J. "Pressure-volume characteristics of dielectric elastomer diaphragms". *In* "Smart Structures and Materials", pages 159–169. International Society for Optics and Photonics (2003)

Tielking J.T. "Analytic tire model. Phase I: The statically loaded toroidal membrane". Technical report, Transportation Research Institute (UMTRI) (1975)

Tiersten H. "Coupled magnetomechanical equations for magnetically saturated insulators". *Journal of Mathematical Physics*, 5(9):1298–1318 (1964)

Tiersten H. "Variational principle for saturated magnetoelastic insulators". *Journal of Mathematical Physics*, 6(5):779–787 (1965)

Treloar L. "Stress-strain data for vulcanised rubber under various types of deformation". *Transactions of the Faraday Society*, 40:59–70 (1944)

Treloar L.R.G. "The photoelastic properties of short-chain molecular networks". *Trans. Faraday Soc.*, 50:881–896 (1954)

Truesdell C. and Toupin R. "The classical field theories. in S. Flügge (ed.), Encyclopedia of physics. principles of classical mechanics and field theory (vol. iii/i)". pages 226–793 (1960)

Verron E. and Marckmann G. "Inflation of elastomeric circular membranes using network constitutive equations". *International Journal of Non-Linear Mechanics*, 38(8):1221–1235 (2003)

Wang F., Yuan C., Lu T., and Wang T. "Anomalous bulging behaviors of a dielectric elastomer balloon under internal pressure and electric actuation". *Journal of the Mechanics and Physics of Solids*, 102:1 – 16 (2017)

Wriggers P. and Taylor R. "A fully non-linear axisymmetrical membrane element for rubber-like materials". *Engineering Computations*, 7(4):303–310 (1990)

Wu C.H. "Plane linear wrinkle elasticity without body force". Technical report, Department of Materials Engineering, University of Illinois, Chicago (1974)

Yang W.H. and Feng W.W. "On axisymmetrical deformations of nonlinear membranes". *Journal of Applied Mechanics*, 37(4):1002–1011 (1970)